AMERICAN SOCIETY FOR MICROBIOLOGY | Molecular and Cellular Biology®

RESEARCH ARTICLE

Adaptation to Endoplasmic Reticulum Stress Requires Transphosphorylation within the Activation Loop of Protein Kinases Kin1 and Kin2, Orthologs of Human Microtubule Affinity-Regulating Kinase

Chandrima Ghosh,[a] Leena Sathe,[a] Joel David Paprocki,[b] Valerica Raicu,[a,b] Madhusudan Dey[a]

[a]Department of Biological Sciences, University of Wisconsin—Milwaukee, Milwaukee, Wisconsin, USA
[b]Department of Physics, University of Wisconsin—Milwaukee, Milwaukee, Wisconsin, USA

ABSTRACT Perturbations in endoplasmic reticulum (ER) homeostasis, a condition termed ER stress, activate the unfolded protein response (UPR), an intracellular network of signaling pathways. Recently, we have shown that protein kinase Kin1 and its paralog, Kin2, in the budding yeast *Saccharomyces cerevisiae* (orthologs of microtubule affinity-regulating kinase in humans) contribute to the UPR function. These Kin kinases contain a conserved kinase domain and an autoinhibitory kinase-associated 1 (KA1) domain separated by a long undefined domain. Here, we show that Kin1 or Kin2 protein requires minimally a kinase domain and an adjacent kinase extension region (KER) for UPR function. We also show that the functional mini-Kin2 protein is predominantly visualized inside the cells and precipitated with the cellular membrane fraction, suggesting its association with the cellular endomembrane system. Furthermore, we show that transphosphorylation of the Kin1 residue T302 and the analogous Kin2 residue T281 within the activation loop are important for full kinase activity. Collectively, our data suggest that, during ER stress, the Kin kinase domain is released from its autoinhibitory KA1 domain and is activated by transphosphorylation.

KEYWORDS protein kinase, Kin1, Kin2, activation loop, phosphorylation, ER stress

In eukaryotic cells, the endoplasmic reticulum (ER) is an intracellular organelle where approximately one-third of cellular proteins fold and mature by sequential action of multiple molecular chaperons (1, 2). Matured proteins are then distributed to other internal organelles, plasma membrane, and/or extracellular space (3). Many of these regular functions are challenged when cells encounter several abiotic and biotic stress conditions, including starvation, hypoxia, and pathogen infections (4). These stress conditions may alter the cellular protein folding processes, causing accumulation of unfolded proteins inside the ER, a state termed ER stress (4). To alleviate ER stress and to maintain protein homeostasis (proteostasis), cells activate a network of signaling pathways collectively called the unfolded protein response (UPR) (5, 6). In mammalian cells, the UPR signaling pathway has been shown to be initiated by three ER-resident proteins, Ire1 (inositol-requiring enzyme 1) (7–9), PERK (protein kinase RNA-like ER kinase) (10), and ATF6 (activating transcription factor-6) (11), whereas in yeast cells, only Ire1 signals the UPR (12).

Each of these ER-resident proteins (Ire1, PERK, and ATF6) contains an ER lumenal domain that senses the ER stress and a cytoplasmic domain that transmits the ER stress signal to cytoplasmic transcriptional activators as follows. Ire1 initiates the UPR signal by cleaving an intron from the translationally repressed *HAC1* mRNA in budding yeast (13–16), *bZIP74* in rice (17), *bZIP60* in thale cress (18), and *XBP1* mRNA in mammalian

Received 23 May 2018 **Returned for modification** 19 June 2018 **Accepted** 18 August 2018

Accepted manuscript posted online 10 September 2018

Citation Ghosh C, Sathe L, Paprocki JD, Raicu V, Dey M. 2018. Adaptation to endoplasmic reticulum stress requires transphosphorylation within the activation loop of protein kinases Kin1 and Kin2, orthologs of human microtubule affinity-regulating kinase. Mol Cell Biol 38:e00266-18. https://doi.org/10.1128/MCB.00266-18.

Copyright © 2018 American Society for Microbiology. All Rights Reserved.

Address correspondence to Madhusudan Dey, deym@uwm.edu.

cells (19, 20). Exons of *HAC1* mRNA are joined by tRNA ligase Rlg1 (21), whereas RtcB ligates exons of *XBP1* mRNA (22). The matured *HAC1*, *bZIP74*, *bZIP60*, or *XBP1* mRNA then yields functional Hac1/bZip74/bZip60/Xbp1 protein. In parallel, PERK phosphorylates the translation initiation factor 2α (eIF2α), leading to activation of the transcription factor Atf4 (23, 24). Unlike Ire1 and PERK, Atf6 itself transmits the stress signal while moving from the ER to the Golgi apparatus, where its transcriptional regulatory domain is activated and released. Collectively, transcription factors Hac1/Xbp1, Gcn4, Atf4, and Atf6 activate the expression of several stress response genes that increases the protein folding capacity of the ER.

Along with the UPR, another stress relief mechanism, termed ER-assisted degradation (ERAD), operates within cells in order to detect and eliminate the unfolded or misfolded proteins. During ERAD, misfolded or unfolded proteins are specifically retrotranslocated to the cytoplasm for subsequent ubiquitylation and degradation by the 26S proteasome (25–27). Finally, both UPR and ERAD operate together to maintain ER proteostasis. However, these UPR and ERAD models cannot explain sufficiently how several newly discovered UPR-related proteins (e.g., Slt2 mitogen-activated protein [MAP] kinase in yeast cells [28] and human p85α regulatory subunit of the phosphoinositide 3 [PI3]-kinase [29, 30]) contribute to ER proteostasis. These discoveries indicate that a highly dynamic and complex UPR network exists to modulate ER proteostasis. Recently, we have shown that high-copy-number protein kinase gene *KIN1* or its paralog, *KIN2*, restores the defective ER-stress response associated with a mutation at the 3′ untranslated region (3′-UTR) of *HAC1* mRNA in the budding yeast *Saccharomyces cerevisiae* (31). Previously, Elbert and coworkers showed that high-copy-number *KIN1* or *KIN2* suppresses the growth defect associated with mutations in several secretory proteins, including mutations in secretory/vacuolar pathway components Sec1 and GTPase Cdc42 (32). Thus, it appears that both Kin1 and Kin2 participate in the control of cellular protein homeostasis, likely by engaging the UPR or by modulating the secretory pathways by unknown mechanisms. Indeed, a very limited number of studies have been done on how Kin kinases contribute independently or additively to either pathway.

Kin1 and Kin2 are members of a family of Ser/Thr kinases consisting of microtubule affinity-regulating kinase (Mark) in humans (33), Par1 (partitioning-defective 1) in worm (34), and Kin1 in fission yeast (35). Kin1/Kin2/Mark/Par1 kinases are known to play important roles in cell polarity (34, 36–38), exocytosis (32), and/or ER stress responses (31). Each protein contains a conserved kinase domain (KD) and an autoinhibitory kinase-associated 1 (KA1) domain separated by a long spacer or undefined domain (Fig. 1A) (31). The kinase domain has been shown to play important roles in overall Kin kinase function either in the secretory pathway (32) or in the ER stress response pathway (31). Thus, it appears that Kin kinases contribute to both secretory and UPR signaling pathways, most likely by constituting an independent signaling cascade or by augmenting the available avenues by which cells adapt to ER stress or secretory demand. However, it is not yet clearly known how Kin kinase domains are activated and how these kinases transmit the secretion or ER stress signal to downstream effector molecules. Here, we show that Kin1 and Kin2 proteins minimally require a KD and an adjacent kinase extension region (KER) for their function both *in vivo* and *in vitro*. We also show that the functional mini-Kin2 protein is predominantly localized within the cytoplasm and precipitated with the cellular membrane fraction, suggesting its association with the cellular endomembrane. Furthermore, we provide *in vivo* and *in vitro* evidence that the Kin2 residue Thr-281 and Kin1 residue Thr-302 within a flexible loop, also known as the activation loop, are phosphorylated in *trans* to activate its kinase domain function.

RESULTS

Both Kin1 and Kin2 proteins require minimally a KD and a KER in adapting to ER stress. Protein kinase Kin2, or its N-terminal region (residues 1 to 526), has been shown to be sufficient to suppress the growth defects of several secretory mutants (32).

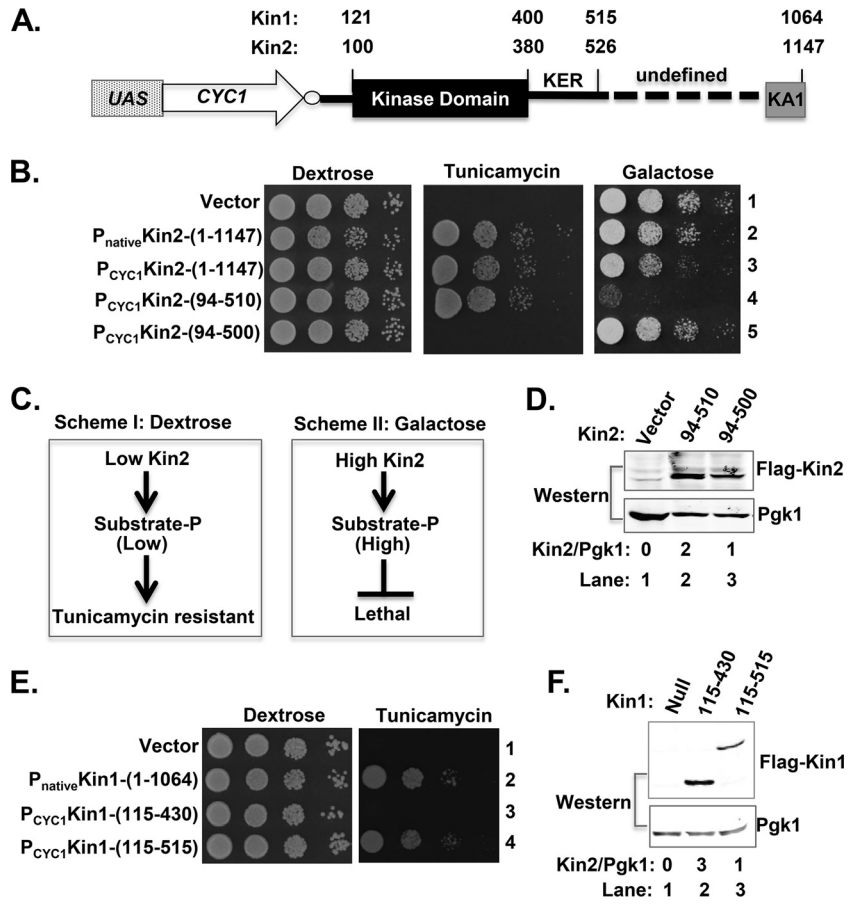

FIG 1 Kin1 and Kin2 proteins require a kinase extension region (KER) for their kinase function. (A) The schematic representation of Kin1 and Kin2 proteins. Both Kin1 and Kin2 are tagged with a Flag epitope (circle) at the N terminus and expressed from a weak *CYC1* promoter containing a galactose-inducible upstream activator sequence (*UAS*). The kinase domain, long spacer (dashed line), newly defined KER, and kinase-associated 1 (KA1) domain are indicated. Numbers on the top indicate amino acid residues for Kin1 and Kin2. (B) Analysis of yeast cell growth. A *kin1*Δ *kin2*Δ strain containing a vector plasmid (null) or expressing a wild-type Kin2 from the native promoter [P_{native}Kin2-(1-1147)] or *CYC1* promoter [P_{CYC1}Kin2-(1-1147)] were grown, serially diluted, spotted, and grown on synthetic dextrose medium, dextrose plus tunicamycin (an ER stress inducer) medium, and galactose medium. *kin1*Δ *kin2*Δ strains expressing truncated Kin2 proteins from the *CYC1* promoter [P_{CYC1}Kin2-(94-510) and P_{CYC1}Kin2-(94-500)] were also tested for their growth on the dextrose, tunicamycin, and galactose media. (C) Schemes for the proposed role of Kin2 and its substrate phosphorylation. On the dextrose medium (scheme I), Kin2 expresses at a low level, leading to a low level of phosphorylation of its substrate and resistance to tunicamycin. On the galactose medium (scheme II), Kin2 expresses at a high level, which phosphorylates its own substrate as well as other unknown proteins promiscuously at a high level, leading to a lethal phenotype. (D) Analysis of Kin2 protein expression. Whole-cell extracts were prepared from yeast cells containing a vector plasmid or indicated Kin2 derivatives (residues 94 to 510 and 94 to 500) and subjected to SDS-PAGE, followed by Western blot analyses using anti-Flag (to detect Kin2) and anti-Pgk1 (to determine the loading control) antibodies. (E) Analysis of yeast cell growth. A *kin1*Δ *kin2*Δ strain expressing full-length Kin1 from its natural promoter [P_{native}Kin1-(1-1064)] and its indicated derivatives from the *CYC1* promoter [P_{CYC1}Kin1-(115-430) and P_{CYC1}Kin1-(115-515)] were grown, serially diluted, spotted, and grown on dextrose and tunicamycin media. (F) Analysis of Kin1 protein expression. Whole-cell extracts were prepared from yeast cells containing a vector plasmid or the indicated Kin1 derivatives (residues 115 to 430 and 115 to 515) and subjected to Western blot analyses using anti-Flag (to detect Kin1) and anti-Pgk1 (to determine the loading control) antibodies.

Recently, we also showed that Kin2 is actively involved in the UPR (31), suggesting that Kin2 plays pleotropic roles in cellular functions. To gain mechanistic insight into how Kin2 contributes to the UPR, we initially determined its optimum length and the relative importance of its constituent domains in ER stress response. We made several Kin2 constructs that lacked the DNA sequences encoding either N-terminal or C-terminal residues (Fig. 1A). Effects of residue deletions were then tested by a functional com-

plementation approach. In this approach, each truncated Kin2 construct was introduced in a *kin1*Δ *kin2*Δ strain from a weak *CYC1* promoter containing a galactose-inducible upstream activator sequence (*Gal-UAS*). The resulting strains were then grown on the medium containing dextrose (to test the functional effect when the candidate protein was expressed at a basal level), dextrose plus 2.0 μg/ml tunicamycin (to test the functional effect when the candidate protein was expressed at a basal level under a condition of ER stress), or galactose (to test the functional effect when the candidate protein was expressed at a high level).

As shown in Fig. 1B, the *kin1*Δ *kin2*Δ strain containing a vector plasmid grew on dextrose medium (row 1) but did not grow on medium containing an ER stress inducer, tunicamycin (row 1). The same strain grew on tunicamycin medium when the vector plasmid expressed full-length Kin2 protein from its native promoter [Fig. 1B, P_{native}Kin2-(1-1147), row 2] or from the weak *CYC1* promoter [Fig. 1B, P_{CYC1}Kin2-(1-1147), row 3]. Western blot analysis showed that the expression of Kin2 protein from the native or *CYC1* promoter was extremely low or undetectable (data not shown). However, the low level of Kin2 expression from either promoter was sufficient to promote growth on the medium containing tunicamycin, likely by phosphorylating its substrate at a low level (Fig. 1C, scheme I, dextrose). Here, we used the promoter *CYC1* containing an upstream *Gal-UAS* activator (i.e., *Gal-UAS* · *CYC1*) to measure the activity of Kin2 kinase. The advantage of the *Gal-UAS* system is that Kin2 protein can be expressed at a relatively high level simply by replacing dextrose with galactose in the culture medium for a few hours (see Materials and Methods). These strategies overcome the Kin2 detection problems associated with its low expression and facilitate the determination of the expression levels of different Kin2 isoforms.

Like a full-length Kin2 protein (residues 1 to 1147), a truncated derivative containing residues 94 to 510 [i.e., Kin2-(94-510)] was able to complement the Kin1 and Kin2 double null strain, thus promoting growth on the tunicamycin medium (Fig. 1B, tunicamycin, compare rows 1 and 4). We also observed that further deletion of as few as 15 residues from the N-terminal end of Kin2-(94-526) [i.e., Kin2-(110-526); data not shown] or 10 residues from the C-terminal end of Kin2-(94-510) [i.e., Kin2-(94-500)] completely abrogated yeast growth on the tunicamycin medium (Fig. 1B, tunicamycin, row 5). Western blot analyses showed that the expression of the Kin2-(94-500) derivative was ~2-fold lower than the expression of Kin2-(94-510) (Fig. 1D, Western, compare lanes 2 and 3 and ratio of Kin2 to Pgk1), suggesting that growth defects were not due to a major change in protein expression and that Kin2 residues 500 to 510 play an important role in stabilizing and/or integrating the protein structure. Collectively, our data suggest that both Kin2-(94-500) and Kin2-(110-526) constructs produced nonfunctional proteins, and Kin2 residues 94 to 510 were minimally required for its normal function.

To further confirm our results, we grew the *kin1*Δ *kin2*Δ yeast strain harboring the full-length Kin2 or its derivatives on galactose medium (Fig. 1B, galactose). We observed that yeast cells expressing full-length Kin2 [i.e., Kin2-(1-1147)] grew on the galactose medium (Fig. 1B, galactose, row 3), whereas cells expressing a truncated Kin2 protein [i.e., Kin2-(94-510)] did not grow on the galactose medium (Fig. 1B, galactose, row 4). We interpret our results in light of a proposed model (Fig. 1C, scheme II, galactose). The KD of the full-length Kin2 is associated with its C-terminal KA1 domain, as reported earlier (32), resulting in an inhibition of its KD function and a normal growth phenotype on galactose medium. In contrast, KD of the truncated Kin2-(94-510) protein is free from such inhibition, which can readily phosphorylate its substrate and promiscuously phosphorylate other cellular proteins at a high level, thereby inhibiting cell growth (Fig. 1C, scheme II, galactose). We also observed that cells expressing the truncated Kin2-(94-500) or Kin2-(110-526) protein grew on galactose medium (Fig. 1B, galactose, row 5, and data not shown). We deduce that Kin2-(110-526) or Kin2-(94-500) derivative lacks kinase activity, likely due to the absence of a few N-terminal or C-terminal residues normally required for its kinase domain that folds into a correct conformation and/or associates with a protein complex in order to be functional inside the cell. Collectively,

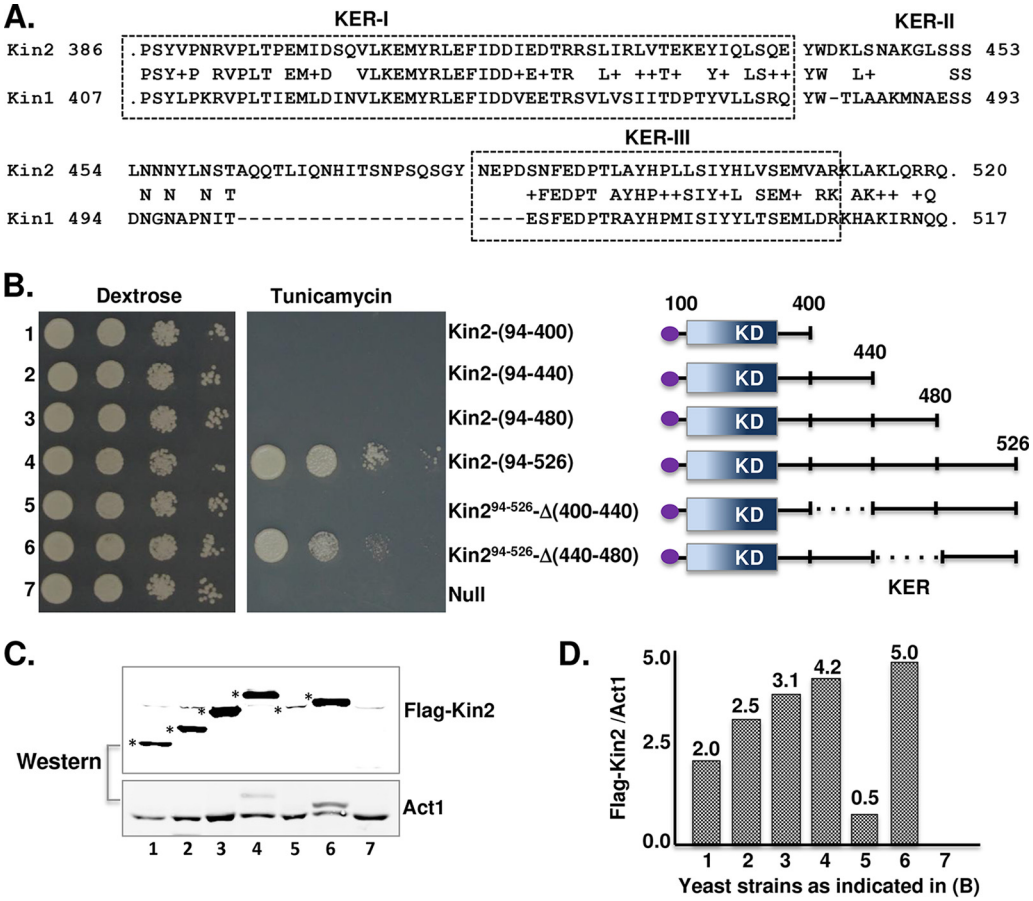

FIG 2 Two distinct regions within the KER control Kin2 kinase function. (A) Comparison of KER sequences in Kin1 and Kin2 proteins. Protein sequences of Kin1 and Kin2 were pairwise aligned. From the sequence alignment, the KER residues of Kin1 (residues 407 to 517) and Kin2 (residues 386 to 520) are shown. Between the two sequences, the conserved residues are shown by letters and the identical residues are shown by plus signs. The putative KER subdomains I and III are shown by boxes. (B) Analysis of yeast cell growth. (Left) The *kin1*Δ *kin2*Δ deletion strains expressing the indicated Kin2 derivatives were tested for growth on dextrose and tunicamycin media. (Right) Schematic representation of Flag epitope (circle)-tagged Kin2 deletion constructs. The kinase domain (KD) and KER (solid line) are shown. The dashed line indicates that the region is deleted. The number indicates residue numbers within the protein. (C) Analysis of Kin2 protein expression. Whole-cell extracts from the indicated yeast cells (as described for panel B) were subjected to SDS-PAGE, followed by Western blot analyses using anti-Flag and anti-actin (Act1) antibodies. The Flag-tagged Kin2 protein bands are indicated by asterisks. (D) The relative expression of Flag-Kin2 protein deletion mutants. The protein band intensities of Flag-tagged Kin2 and Act1 were measured using ImageJ software. The ratios of Flag-Kin2 and Act1 are represented in a bar diagram.

these data further confirm that Kin2 residues 94 to 510 are minimally required for its kinase function.

The BLAST search of Kin2 residues 94 to 510 showed that residues 100 to 380, as expected, had significant homology (31% identities, 52% positives, and 12% gaps) with a classical protein kinase domain of protein kinase A (PKA) with a conserved Lys-128 (K128) in the VAIK motif and a catalytic Asp-248 (D248) in the HRD motif (39). In contrast, residues 380 to 510 had no detectable homology to any conserved protein domain family except with residues 425 to 515 of Kin1 protein (Fig. 2A). Thus, it appears that residues 386 to 510 in Kin2 or residues 407 to 515 in Kin1, here referred to as the KER, play an important role in kinase domain function. We next determined the relative importance of KER in Kin1 protein.

We made two truncated Kin1 constructs expressing (i) Kin1 residues 115 to 430, containing only the KD, and (ii) the Kin1 residues 115 to 515, containing both the KD and KER domain. Both Kin1-(115-430) and Kin1-(115-515) constructs were introduced in a *kin1*Δ *kin2*Δ strain (Fig. 1E). The resulting strains were tested for their growth on dextrose and tunicamycin media (Fig. 1E). As shown in Fig. 1E, the *kin1*Δ *kin2*Δ strain

containing a vector plasmid was unable to grow on tunicamycin medium (row 1) but was able to grow on the same medium when the vector plasmid harbored the full-length *KIN1* gene [i.e., Kin1-(1-1064)] under its native promoter (row 2). The *kin1*Δ *kin2*Δ strain also grew on the tunicamycin medium when it expressed a truncated Kin1 protein composed of residues 115 to 515 [i.e., Kin1-(115-515)] from a weak *CYC1* promoter containing the *Gal-UAS* activator (Fig. 1E, row 4, and F, Western, lane 3). However, the *kin1*Δ *kin2*Δ strain was unable to grow on the tunicamycin medium when it expressed a truncated Kin1 protein consisting of residues 115 to 430 [i.e., Kin1-(115-430)] (Fig. 1E, tunicamycin, row 3, and F, Western, lane 2). Indeed, Western blot analysis showed that the expression of Kin1-(115-430) derivative was ~3-fold more than the expression of Kin1-(115-515) (Fig. 1F, Western, compare lanes 2 and 3). However, these data suggested that the growth defect was due to expression of a nonfunctional Kin1 kinase domain. From these results, it appeared that Kin1 residues 115 to 515, like Kin2 residues 94 to 510, were minimally required for its function. Here, we refer to the mini-functional Kin1 and Kin2 proteins as Kin1^{mini} (i.e., Kin1 residues 115 to 515) and Kin2^{mini} (i.e., Kin2 residues 94 to 526), respectively.

Two distinct regions in Kin2-KER control Kin2^{mini} function. Pairwise alignment of Kin1 and Kin2 protein sequences revealed that Kin1 residues 463 to 482 had little homology with Kin2 residues 442 to 462 (30% identities) (Fig. 2A). It also revealed that Kin1 lacked 23 residues corresponding to Kin2 residues 464 to 485 (Fig. 2A). Based on these findings, we proposed that KER of Kin2 was composed of three separate subdomains: KER-I (residues 386 to 440), KER-II (residues 440 to 480), and KER-III (residues 480 to 510). Further, BLAST search with the small peptide sequences of each subdomain revealed that KER-I showed partial protein sequence homology with the ubiquitin-associated (UBA) domain of several proteins, including a human autophagy protein, Nbr1 (40), and a human Kin2 ortholog, Mark3 (41). This computational analysis suggested that the KER-I subdomain adopts a UBA-like domain, and KER-II and -III subdomains might play an unknown role in kinase domain function. We investigated the relative physiological importance of the proposed subdomains by deletion analyses.

A series of deletion mutants were created by systematically removing each KER subdomain from the Kin2^{mini} protein. As shown in Fig. 2B (right), we generated three Kin2^{mini} constructs by consecutively deleting DNA sequences encoding 40 residues from the C-terminal end [e.g., Kin2-(94-480), Kin2-(94-440), and Kin2-(94-400)] and two Kin2^{mini} constructs by deleting DNA sequences encoding 40 residues from the internal region [e.g., Kin2^{mini}-Δ(400-440) and Kin2^{mini}-Δ(440-480)]. Each of these derivatives was then introduced into a *kin1*Δ *kin2*Δ strain, and the resulting strains were tested for their growth on dextrose and dextrose plus tunicamycin media (Fig. 2B). As shown in the Fig. 2B, yeast cells containing Kin2^{mini}-Δ(440-480), like Kin2^{mini}, grew on tunicamycin medium (tunicamycin, rows 4 and 6), suggesting that Kin2^{mini}-Δ(440-480) expressed a functional protein. In contrast, yeast cells containing the Kin2-(94-480), Kin2-(94-440), Kin2-(94-400), and Kin2^{mini}-Δ(400-440) alleles were unable to grow on tunicamycin medium (Fig. 2B, tunicamycin, rows 1, 2, 3, and 5). Western blot analysis showed that each of those Kin2 deletion derivatives were expressed in yeast cells (Fig. 2C, Western, lanes 1, 2, and 3), albeit at various levels and at an exceptionally low level for Kin2^{mini}-Δ(400-440) protein (Fig. 2C, lane 5, and D, comparative ratio analyses of Kin2 and Act1 protein bands). These data suggested that growth defects were not due to a major lack of protein expression but to expression of nonfunctional proteins. From these results, it appears that Kin2 residues 440 to 480 (i.e., KER-II) play a redundant role, whereas residues 400 to 440 (i.e., KER-I) and 480 to 526 (i.e., KER-III) separately modulate the Kin2^{mini} function either by stabilizing the closed conformation of the KD, as observed in typical kinases, including the human Mark3 (41), or by controlling the catalytic activity of the KD, as observed in Ca^{2+}/calmodulin-dependent protein kinase 1 (42).

KER-I sequences of Kin1 and Kin2 are partially similar to the UBA-like domain sequences of human Mark3 and Nbr1 proteins. The UBA-like domain in Mark3 has been

shown to bind the N-terminal lobe of the kinase domain (41), implicating it in having a role in integrating and stabilizing the kinase domain. The UBA-like domain in Nbr1 appears to be a negative regulator of Nbr1 function, where an alanine mutation of the conserved leucine residue (i.e., L954) impairs the binding of ubiquitin (40). However, the spatial arrangement of three constituent α-helices in the Mark3-UBA domain is different from the spatial arrangement of three constituent helices in the Nbr1-UBA domain (41). Thus, it is still uncertain how KER-I functions independently and/or additively with other domains in the same protein in order to regulate its kinase domain function. While dimerization and activation at the membrane is a common intermediate for many kinases, including Src family kinase (43), it is reasonable to assume that Kin2-KER plays an important role in membrane anchorage and/or dimerization, likely by associating with other membrane-binding factors.

Kin2^{mini} is an endomembrane protein. Tibbetts and coworkers have shown that Kin kinases precipitate with the membrane fraction (44), indicating that Kin kinases are associated with the plasma and/or organelle membranes. Previously we have shown that, under conditions of ER stress, both green fluorescent protein (GFP)-Kin2 and GFP-Kin2$^{\Delta KA1}$ fusion proteins were predominantly visualized as discrete dots within the cytoplasm (31). Recently, Yuan et al. showed that the GFP-fused full-length Kin2 protein is localized at sites of polarized growth within the bud neck/tip (45). They also show that the GFP–Kin2-(1-526) fusion protein is localized at the bud tip (45). Based on those observations, they propose that two distinct regions in Kin2 protein determine its localization. Thus, it was reasonable to assume that the functional Kin2^{mini} is a membrane-anchoring protein, and we investigated the cellular localization of Kin2^{mini} protein.

We generated a GFP2-Kin2^{mini} fusion protein construct under the Kin2 native promoter in which the coding sequence of a monomeric A206K green fluorescence protein, GFP2 (46), was inserted at the N-terminal end of the Kin2^{mini} protein coding sequence. The GFP2-Kin2^{mini} fusion protein, like the wild-type Kin2^{mini} protein, complemented the *kin1*Δ *kin2*Δ strain and allowed yeast cells to grow on the tunicamycin medium (data not shown), suggesting that GFP2-Kin2^{mini} was a functional protein. The GFP2-Kin2^{mini} fusion protein then was introduced into a strain lacking a transmembrane protein, Ste2 (i.e., *ste2*Δ strain). The *ste2*Δ strain containing GFP2-Kin2^{mini} was retransformed with a plasmid expressing the Ste2-YFP (yellow fluorescent protein) fusion protein (46). The *ste2*Δ strain coexpressing both GFP2-Kin2^{mini} and Ste2-YFP was used for imaging studies by a two-photon microscope in the presence and absence of an ER stressor, dithiothreitol (DTT) (see Materials and Methods). As expected, more than 60 to 70% of cells showed the YFP signals at the edge of cells because of the membrane localization of Ste2 protein (Fig. 3A). The same cells predominantly showed the GFP2 signals inside the cytoplasm (Fig. 3A). Moreover, we observed that overall GFP2 signal was 60% stronger when cells were treated with DTT (Fig. 3B). Thus, our data suggested that Kin2^{mini} localizes predominantly inside the cytoplasm.

To determine whether or not Kin2^{mini} protein was associated with cellular endomembrane, we then prepared the whole-cell extract from a *kin1*Δ *kin2*Δ strain expressing Flag-Kin2^{mini} and separated soluble and insoluble fractions by centrifugation at 20,000 $\times$ *g* (see Materials and Methods). Both soluble and insoluble fractions were subjected to SDS-PAGE and Western blot analysis using an anti-Flag antibody to detect Flag-Kin2 protein, an anti-Hac1 antibody to detect a soluble cytoplasmic protein, and an anti-Kar2 antibody to detect an ER-resident and membrane-associated chaperone. As expected, the majority of Hac1 protein was detected in the soluble fraction, whereas the majority of Kar2 was detected with the insoluble fraction (Fig. 3C, lane 2). A small fraction of Kar2 was also observed in the soluble fraction (Fig. 3C, lane 3), suggesting that a fraction of Kar2 protein was released from the membranes and/or the centrifugation at 20,000 $\times$ *g* partially precipitated the cellular membranes. Interestingly, we observed that the majority of Kin2^{mini} protein was separated with the insoluble

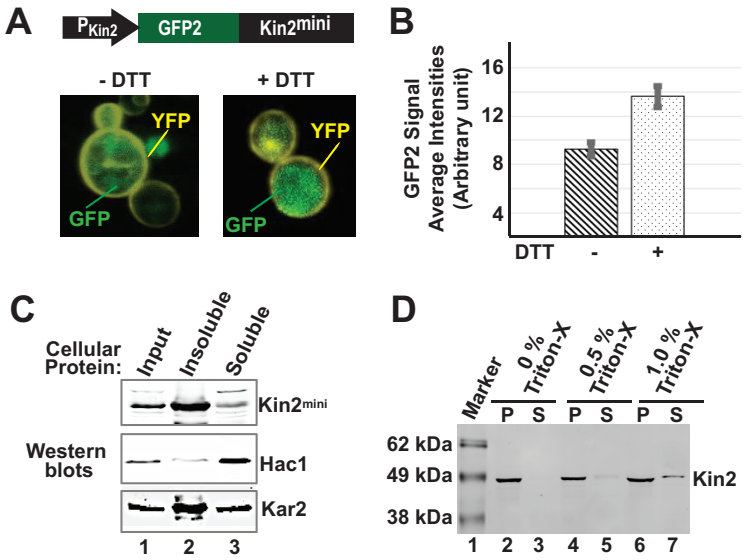

FIG 3 Kin2^{mini} is likely associated with cellular endomembrane. (A) GFP2-fused Kin2^{mini} protein is visualized inside the cells. (Top) Open reading frame of GFP2 and Kin2^{mini} fused and expressed from the Kin2 native promoter. (Lower) GFP2-fused Kin2^{mini} protein was expressed in a *ste2*Δ cell harboring an Ste2-YFP fusion protein. The GFP and YFP signals were detected by two-photon microscopy and are shown by arrows. (B) Quantification of relative expression of GFP2 signals. The relative expression of GFP2 signal in the presence (+) and absence (−) of an ER stressor, DTT, was measured as described in Materials and Methods. The average intensities ± weighted errors are represented as arbitrary units. (C) Kin2^{mini} protein associates with the membrane fraction. Yeast cell extract containing the Flag-tagged Kin2^{mini} protein was separated by centrifugation as soluble and insoluble membrane fractions (see Materials and Methods). Both fractions were subjected to SDS-PAGE and Western blot analysis using an anti-Flag antibody to detect Kin2, anti-Hac1 antibody to detect soluble protein, and anti-Kar2 antibody to detect an insoluble ER membrane-resident protein. (D) Triton X-100 partially solubilizes Kin2^{mini} protein from the membrane fraction. Yeast cell extract containing the Flag-tagged Kin2^{mini} protein was separated as soluble and insoluble membrane fractions. The insoluble fraction was mixed with 0.5 or 1% Triton X-100 to solubilize the membrane-bound proteins. The pellet (P) and supernatant (S) fractions were separated by centrifugation and subjected to SDS-PAGE and Western blot analysis using an anti-Flag antibody to detect Kin2 protein.

fractions along with the Kar2 protein (Fig. 3C, upper, lanes 2 and 3). These data suggest that Kin2^{mini} is a membrane-associated protein.

To rule out the possibility that the membrane association was not a result of deposition of Kin2 inclusion bodies on the membrane, we treated the membrane fraction containing Kin2^{mini} with 0.5 or 1% Triton X-100 to the break the lipid-lipid and lipid-protein interactions and to solubilize the membrane proteins. The soluble proteins were then separated from the pellet by centrifugation at 20,000 × *g*. Both soluble and pellet fractions then were subjected to Western blot analysis. In the Western blot, we observed a significant amount of Kin2 protein in the 0.5% or 1% Triton X-100 solubilized fraction (Fig. 3D, lanes 5 and 7), suggesting that Kin2^{mini} protein was associated with membrane, not precipitated as an inclusion body. Taken together, our data suggest that Kin2^{mini}, like full-length Kin2, is an endomembrane kinase.

Activation loop phosphorylation is important for kinase activity of Kin2^{mini}. The *Saccharomyces* Genome Database (SGD) shows that protein kinases Kin1 and Kin2 are phosphorylated at more than 30 serine, threonine, and tyrosine residues (some of which are common in both proteins), indicating that these kinases are regulated by a complex mechanism involving auto- and/or transphosphorylation. Here, we investigated how the phosphorylated residues regulated the Kin2 kinase function. Initially, we determined how many of these reported residues were phosphorylated in the Kin2^{mini} protein under conditions of ER stress. Thus, we purified Kin2^{mini} protein from cells grown under conditions of ER stress and analyzed protein phosphorylation by mass spectrometry. The mass spectral analysis identified three major phosphorylated pep-

tides with phosphorylated residues S151 (peptide 1), Y275 and T281 (peptide 2), and S328 and S329 (peptide 3) (see Materials and Methods).

Typically, the standard mass spectrometry analysis may detect peptides that are phosphorylated at low stoichiometry, which may be meaningless. Indeed, many studies have reported that many mapped phosphorylation sites have little or no effect on physiological function or phenotype. Therefore, it is simply not productive to mutate all phosphorylation sites and test their impact. We assume that if any phosphorylation site is physiologically important, it should be detected in both Kin1 and Kin2 proteins. Thus, we compared the reported phosphorylation sites between Kin1 and Kin2 proteins and identified only 18 phosphorylated residues common in both proteins. Among these 18 residues, two are mapped at the N terminus of the kinase domain (residues S24 and T26), five at the kinase domain (residues S151, Y275, T281, S328, and S329), and 11 at the undefined domain (residues T577, T608A, S609, S612, T629, S663, S706, S714, S1020, T1031, and T1037).

To determine how the putative 18 phosphorylated residues influenced Kin2 kinase function, we initially focused our studies on the Kin2^{mini} protein. These residues were mutated to nonphosphorylatable alanine (singly or in combination), and mutated proteins were expressed in the *kin1*Δ *kin2*Δ strain. We found that mutations of 11 residues at the regulatory domain by alanine in a single protein (i.e., Kin2-11Ala) did not affect the ability of full-length Kin2 to support cell growth on the tunicamycin medium (data not shown). We also found that a single mutation of residue S151 or double mutation of residues S328 and S329 within the kinase domain by alanine in the Kin2^{mini} protein (i.e., Kin2^{mini}-S151A or Kin2^{mini}-S328A,S329A) did not impair yeast cell growth on the tunicamycin medium (data not shown). These data suggest that phosphorylated residues S151, S328, S329, T577, T608A, S609, S612, T629, S663, S706, S714, S1020, T1031, and T1037 have insignificant impact on the ER stress response.

We next focused on residues Y275 and T281 in the Kin2 protein, which are mapped within a flexible loop (also known as the activation loop) located between the conserved DFG and APE motifs (47). Residues corresponding to Y275 and T281 in Kin2 are residues Ser296 (S296) and Thr302 (T302) in Kin1 (Fig. 4A). To determine the physiological relevance of Y275 or T281 phosphorylation, we individually mutated each one to alanine, generating Kin2^{mini}-Y275A and Kin2^{mini}-T281A constructs in the *Gal4-UAS* hybrid system. Kin2^{mini}-Y275A and Kin2^{mini}-T281A constructs were separately introduced in a *kin1*Δ *kin2*Δ strain. The resulting strains were then tested for growth on dextrose, tunicamycin, and galactose media. As shown in Fig. 4B, cells expressing Kin2^{mini}-Y275A (row 5), like wild-type Kin2^{mini} (row 2), grew on the tunicamycin medium but did not grow on the galactose medium (row 5). Similarly, cells expressing Kin2^{mini}-T281A grew on the tunicamycin medium (Fig. 4B, tunicamycin, row 6). However, cells expressing Kin2^{mini}-T281A grew moderately on galactose medium (Fig. 4B, galactose, row 6). These growth phenotypes suggested that Kin2^{mini}-Y275A and Kin2^{mini}-T281A expressed functional kinases, the alanine mutation of Y275 or T281 did not impair the kinase activity, and the phosphorylation at either residue played an insignificant role under physiological conditions. Alternatively, phosphorylation sites may act in combinatorial mechanisms, phosphorylation at Y275 might compromise the loss of phosphorylation at T281, or vice versa.

To test these possibilities, we mutated both residues Y275 and T281 to alanine in a single protein, generating a Kin2^{mini}-Y275A,T281A mutant. We also mutated both residues Y275 and T281 to glutamate in order to generate phosphomimetic substitutions (i.e., Kin2^{mini}-Y275A,T281E and Kin2^{mini}-Y275E,T281A). These Kin2^{mini}-Y275A,T281A, Kin2^{mini}-Y275E,T281A and Kin2^{mini}-Y275A,T281E mutants were then separately expressed in a *kin1*Δ *kin2*Δ strain. We observed that the *kin1*Δ *kin2*Δ cell expressing Kin2^{mini}-Y275A,T281A mutant protein, like kinase-dead mutants Kin2^{mini}-K128R (K128 is the Lys of the VAIK motif) and Kin2^{mini}-D248A (D248 is the catalytic Asp of the HRD motif), did not grow on the tunicamycin medium (Fig. 4B, tunicamycin, compare rows 3, 4, and 7, and C, Western, lanes 3, 4, and 7) but grew on the galactose medium (Fig. 4B, galactose, compare rows 3, 4, and 7). These data

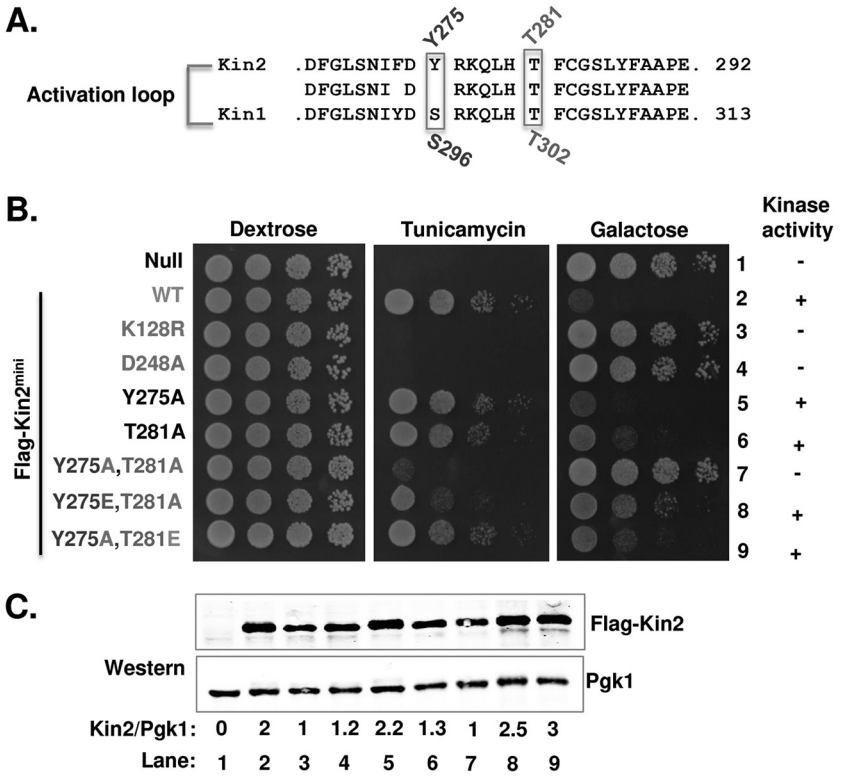

FIG 4 Activation loop phosphorylation is important for Kin2^{mini} kinase activity. (A) Comparison of the activation loop sequences of Kin1 and Kin2 kinases. The activation loop sequences of Kin1 (residues 287 to 313) and Kin2 (residues 267 to 292) were aligned. The phosphorylated residues are indicated on the top for Kin2 or on the bottom for Kin1. (B) Analysis of yeast cell growth. The *kin1*Δ *kin2*Δ deletion strains containing a vector plasmid (null) or expressing wild-type Kin2^{mini} (WT) and its indicated derivatives were tested for growth on dextrose, tunicamycin, and galactose media. Kinase activity is indicated by plus (active) or minus (inactive) signs. (C) Analysis of Kin2 protein expression. Whole-cell extracts prepared from the yeast cells indicated in panel B were subjected to SDS-PAGE, followed by Western blot analyses using anti-Flag and anti-Pgk1 antibodies. The relative expression levels (ratio of Flag-Kin2 and Pgk1 protein band intensities) are indicated at the bottom.

suggested that Kin2^{mini}-Y275A,T281A expressed a nonfunctional protein, similar to the catalytically inactive Kin2-K128R and Kin2-D248A mutants. Interestingly, we observed that the *kin1*Δ *kin2*Δ cells expressing the Kin2^{mini}-Y275E,T281A or Kin2^{mini}-Y275A,T281E mutant protein, like the wild-type Kin2^{mini}, grew on the tunicamycin medium (Fig. 4B, tunicamycin, rows 2, 8, and 9, and C, Western, lanes 2, 8, and 9) and exhibited a lethal phenotype on the galactose medium (Fig. 4B, galactose, compare rows 2, 8, and 9). These *in vivo* data suggested that Kin2^{mini}-Y275E,T281A and Kin2^{mini}-Y275A,T281E expressed active kinases in which glutamate substitutions for Y275 and T281 mimicked the active phosphorylated state. Taken together, these data suggested that activation loop phosphorylation is important for Kin2^{mini} kinase activity.

Activation loop phosphorylation is important for full kinase activity of Kin2. We next investigated the importance of activation loop phosphorylation in a full-length Kin2 protein. A *kin1*Δ *kin2*Δ strain was separately transformed with an empty vector and the same vector bearing a wild-type (WT) *KIN2* gene under its native promoter. Indeed, we engineered the *KIN2* gene to express a Flag epitope at its N-terminal end. Transformants were streaked on both dextrose and tunicamycin media (Fig. 5). As shown in Fig. 5, transformants with the vector plasmid were able to grow on the dextrose medium but were unable to grow on the tunicamycin medium. However, the *kin1*Δ *kin2*Δ cells containing the same plasmid bearing a Flag-tagged Kin2 gene were able to grow on both dextrose and tunicamycin media (Fig. 5A). These data suggested that the Flag tag at the N-terminal end of Kin2 protein had no impact on its kinase function. We

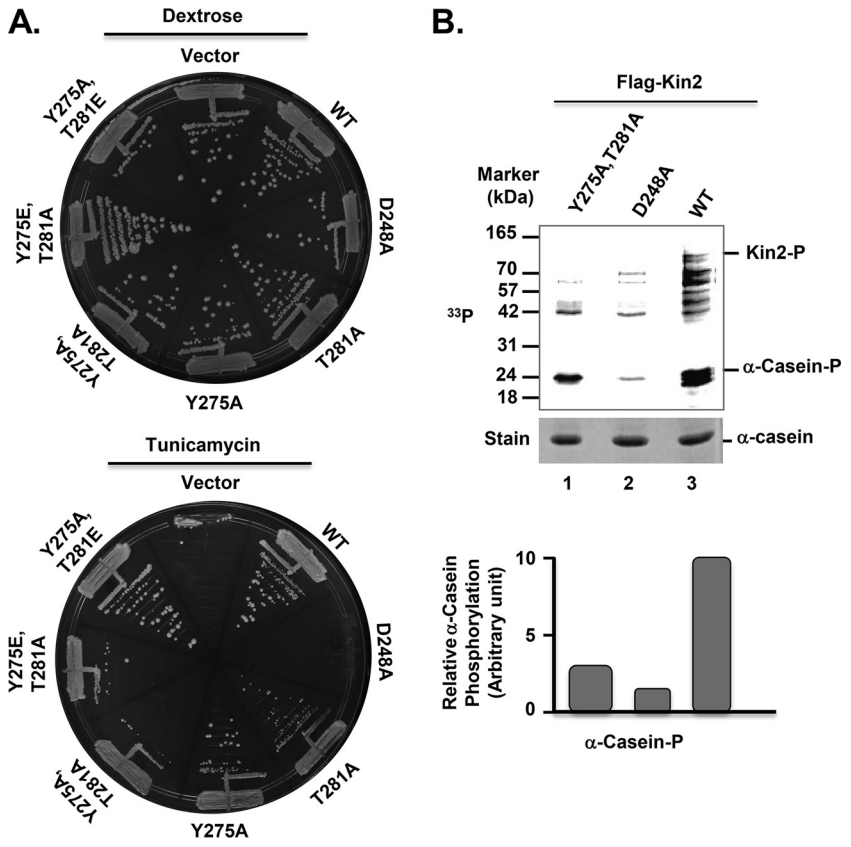

FIG 5 Activation loop phosphorylation is required for full Kin2 kinase function. (A) Analysis of yeast cell growth. The *kin1*Δ *kin2*Δ deletion strains containing a vector plasmid (null) or the same vector plasmid bearing wild-type Flag-Kin2 (WT) or its indicated derivatives were streaked on dextrose (upper) and tunicamycin (lower) media. Cells were then grown at 30°C for 48 h. (B) Analysis of Kin2 kinase activity *in vitro*. Whole-cell extracts (~10 mg) were prepared from the *kin1*Δ *kin2*Δ deletion strains expressing wild-type Flag-Kin2 (WT) and the indicated Kin2 derivatives mixed with anti-Flag M2-agarose beads. The Flag-tagged Kin2 proteins were precipitated, washed with kinase buffer, and mixed with α-casein (0.5 μg) and [γ-^{33}P]ATP (1 μCi). The reaction mixture was then mixed with 2× SDS dye, heated at 90°C for 1 min, centrifuged, and loaded on SDS-PAGE. The gel was stained, dried, and autoradiographed; top. The α-casein protein bands are shown in the middle panel. Incorporation of ^{33}P into α-casein was determined by the relative band intensities and is shown as a bar diagram in the bottom panel.

next mutated the catalytic residue Asp-248 of Flag-Kin2 protein, generating a kinase-inactive Kin2-D248A mutant. We also mutated the phosphorylated residues Y275 and T281 to generate several activation loop mutants (e.g., Kin2-Y275A, Kin2-T281A, Kin2-Y275A-T281A, Kin2-Y275E-T281A, and Kin2-Y275A-T281E). These Kin2 mutants were separately introduced in the *kin1*Δ *kin2*Δ strain, and the resulting strains were tested for growth on both dextrose and tunicamycin media (Fig. 5A).

As shown in Fig. 5A (lower), the *kin1*Δ *kin2*Δ strain containing a kinase-inactive Flag–Kin2-D248A mutant was sensitive to tunicamycin, like the strain containing a vector plasmid, whereas the *kin1*Δ *kin2*Δ strain containing the Flag–Kin2-Y275A-T281E mutant was resistant to tunicamycin, like the strain containing wild-type Flag-Kin2. The resistance to tunicamycin was reduced when the *kin1*Δ *kin2*Δ cells contained a Flag–Kin2-Y275A or Flag–Kin2-T281A mutant (Fig. 5A). This tunicamycin resistance was noticeably further reduced when the *kin1*Δ *kin2*Δ cells contained a Flag–Kin2-Y275A-T281A or Flag–Kin2-Y275E-T281A mutant. We were unable to detect the Flag-Kin2 protein by Western blotting in the whole-cell extract containing 100 μg of total protein, likely due to its low expression from the native promoter (data not shown). However, the obvious ER stress-resistant growth phenotype suggested that the kinase domain function was important to activate the ER stress response, and the activation loop phosphorylation was important for full Kin2 kinase activity. Moreover, we found that

the tunicamycin-resistant phenotypes of *kin1*Δ *kin2*Δ cells containing the Flag–Kin2-Y275A-T281E derivative were comparable to those of cells containing wild-type Flag-Kin2 (Fig. 5A, tunicamycin, lower). These data suggested that phosphorylation at residue T281 plays a major role in kinase domain function.

To further confirm that the activation loop phosphorylation was important for the full kinase activity of Kin2, we performed *in vitro* kinase assays. Approximately 10 mg of total cellular proteins from the *kin1*Δ *kin2*Δ cells expressing Flag–Kin2-WT, Flag–Kin2-D248A, or Flag–Kin2-Y275A-T281A were immunoprecipitated by anti-Flag M2-agarose. The immunoprecipitated proteins were washed with 2× kinase buffer and mixed with α-casein (0.5 μg) and [γ-^{33}P]ATP (1 μCi per reaction mixture) essentially as described previously (48). After 30 min, 2× SDS dye was added to the reaction mixture to quench the kinase reaction. The reaction mixture was then heated at 90°C for 1 min and loaded in an SDS-PAGE gel to separate the α-casein- and M2-agarose-precipitated proteins. The gel was stained to visualize the α-casein protein (Fig. 5B, middle, stain), dried, and autoradiographed (Fig. 5B, ^{33}P).

As shown in the Fig. 5B, a number of phosphorylated protein bands, with molecular masses ranging from 42 to 150 kDa, appeared in the reaction mixture containing WT Flag-Kin2 (lane 3), suggesting that Flag-Kin2 (molecular mass of Kin2 is 128.36 kDa) or other kinases (if any) are autophosphorylated or they in turn phosphorylated other proteins in the immunoprecipitates. We also observed that α-casein was phosphorylated ~10-fold more in the reaction mixture containing the WT Flag-Kin2 protein than the reaction mixture containing the kinase-inactive Flag–Kin2-D248A protein (Fig. 5B, compare lanes 2 and 3, and lower). Flag–Kin2-D248A is an inactive kinase, suggesting that a low level of phosphorylation in α-casein occurs by unknown kinases present in the immunoprecipitates. Moreover, we observed significant α-casein phosphorylation in the reaction mixture containing the Flag–Kin2-Y275A-T281A (Fig. 5B, lane 1) mutant, suggesting that Y275A and T281A mutations in a single protein did not completely abolish the kinase domain function. The relative phosphate incorporation in α-casein showed that Flag–Kin2-Y275A-T281A mutant phosphorylated α-casein ~4-fold less efficiently than WT Flag-Kin2 (Fig. 5B, top and middle compare lanes 1 and 3, and bottom). We were unable to detect the expression of Flag-Kin2 protein by Western blotting due to its extremely low expression. Nonetheless, the ability of the Flag–Kin2-Y275A-T281A mutant to phosphorylate α-casein, albeit less efficiently, suggested that Flag–Kin2-Y275A-T281A mutant expressed a functional protein with a weaker kinase activity, and the activation loop phosphorylation was important for the full kinase activity of Kin2.

Activation loop phosphorylation is important for Kin1^{mini} kinase activity. The Kin2 residues Y275 and T281 correspond to Kin1 residues S296 and T302. Thus, we investigated whether substitution of glutamate for T302 activated the kinase function of Kin1^{mini} protein. We expressed Kin1^{mini} and its derivatives, Kin1^{mini}-D269A (kinase-inactive mutant), Kin1^{mini}-S296A,T302A (nonphosphorylatable mutant), Kin1^{mini}-S296A,T302E, and Kin1^{mini}-S296E,T302A (phospho-mimetic mutants), in a *kin1*Δ *kin2*Δ strain (Fig. 6A). As shown in Fig. 6A, the *kin1*Δ *kin2*Δ strain containing a vector plasmid was unable to grow on the tunicamycin medium (row 1) but was able to grow on the same medium when the vector plasmid contained a WT *KIN1^{mini}* gene (row 2). The *kin1*Δ *kin2*Δ strain containing the Kin1^{mini}-S296A,T302E mutant, like WT Kin1^{mini}, was able to grow on the tunicamycin medium (Fig. 6A, tunicamycin, compare rows 2 and 5). In contrast, the *kin1*Δ *kin2*Δ strain containing the Kin1^{mini}-D269A, Kin1^{mini}-S296A,T302A, or Kin1^{mini}-S296E,T302A mutants, like the vector control, was unable to grow on the tunicamycin medium (Fig. 6A, tunicamycin, rows 1, 3, 4, and 6). Western analysis showed that all of the mutant proteins were expressed at levels comparable to those of the WT, except Kin1^{mini}-S296A,T302E (Fig. 6B, Western, lanes 1 to 6), suggesting that Kin1^{mini}-D269A, Kin1^{mini}-S296A,T302A, and Kin1^{mini}-S296E,T302A mutants expressed nonfunctional kinases. These data further suggested that Kin1^{mini}-S296A,T281E expressed an active kinase in which the glutamate substi-

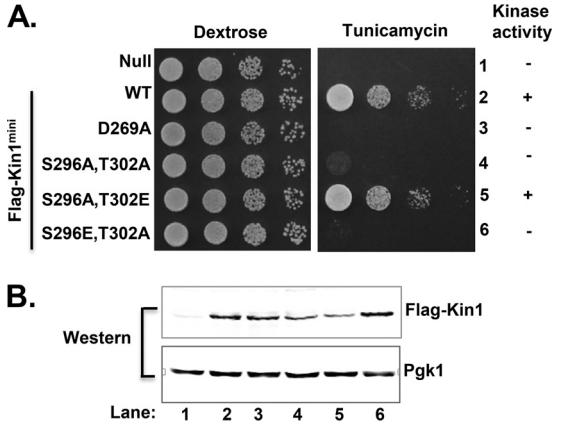

FIG 6 Activation loop phosphorylation is important for Kin1^{mini} kinase activity. (A) Analysis of yeast cell growth. The *kin1*Δ *kin2*Δ deletion strains containing a vector plasmid (null) or expressing wild-type Flag-Kin1 (WT) and the indicated derivatives were tested for their growth on dextrose and tunicamycin media. Kinase activity is indicated as plus (active) or minus (inactive) signs. (B) Analysis of Kin1 protein expression. Whole-cell extracts from the yeast cells indicated in panel A were subjected to SDS-PAGE, followed by Western blotting using anti-Flag and anti-Pgk1 antibodies.

tution for T302 mimicked a phosphorylated residue. It should be noted that the phosphomimetic substitution at the Kin1 residue S296 (i.e., Kin1^{mini}-S296E,T302A), unlike the Kin2 residue Y275 (i.e., Kin2^{mini}-Y275E,T281A) (Fig. 4B, tunicamycin, row 8), was unable to promote growth on the tunicamycin medium (Fig. 6A, tunicamycin, row 6). These observations suggest that the glutamate substitution S296E did not mimic the phosphorylated state or that phosphorylation of S296 had only a minor role for Kin1 kinase activity. Taking these findings together, it appears that phosphorylation of T302 in Kin1 or the corresponding T281 in Kin2 is important for full Kin1 or Kin2 kinase domain function.

Phosphorylation of residue T302 in Kin1 or T281 in Kin2 occurs in *trans*. Most protein kinase domains remain in an inactive state and are activated when cells need them. The inactive-to-active transition in most cases requires phosphorylation within its activation loop (49). Phosphorylation of the activation loop can occur by itself (i.e., autophosphorylation) or may occur via other kinases (i.e., transphosphorylation) or both (50). To determine how T281 phosphorylation occurs in cells, two catalytically inactive kinase mutants (i.e., Kin2^{mini}-D248A and Kin2^{mini}-K128R) were expressed in a *kin1*Δ *kin2*Δ strain (Fig. 7A), and then we examined the phosphorylation status of the T281 residue. Western blot analysis showed that expression of Kin2^{mini}-K128R (Fig. 7A, lower, lane 3) and Kin2 ^{mini}-D248A (Fig. 7A, lower, lane 4) was almost similar to that of wild-type Kin2^{mini} protein (Fig. 7A, lower, lane 2). It should be noted that kinase-inactive Kin2^{mini}-K128R and Kin2 ^{mini}-D248A proteins migrated faster than the respective wild-type protein (Fig. 7A, lower, compare lanes 2, 3, and 4) for unknown reasons. Interestingly, however, we observed that the residue T281 was phosphorylated in both Kin2^{mini}-K128R and Kin2^{mini}-D248A kinase-inactive proteins (Fig. 7A, Western, upper, lanes 3 and 4). We also observed that the level of T281 phosphorylation in Kin2^{mini}-K128R or Kin2^{mini}-D248A (more prominent) was much lower than that in the Kin2^{mini} protein (Fig. 7A, upper, compare lanes 2, 3, and 4). A low level of T281 phosphorylation in Kin2^{mini}-K218R and Kin2^{mini}-D248A can be interpreted by their susceptibility to dephosphorylation by unknown phosphatases, as suggested by Cameron et al. based on their similar observations with protein kinase C (51). Alternatively, the decreased T281 phosphorylation in the kinase-defective mutants may arise from different degrees of compromised autophosphorylation in the K128R and D248A mutants. The phosphorylation of T281 residue in kinase-dead mutants suggested that T281 phosphorylation occurred in a *trans* mechanism by an upstream kinase.

To determine that Kin2^{mini}-K128R was an inactive kinase, we induced the expression of Flag-Kin1^{mini}, Flag–Kin2^{mini}, and Flag-Kin2^{mini}-K128R proteins in yeast *Saccharomyces*

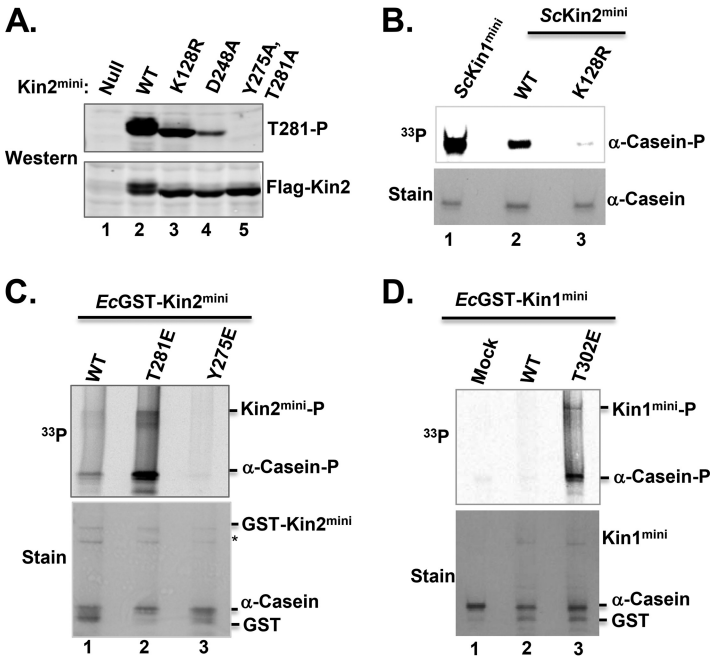

FIG 7 Phosphorylation of Kin2-T281 or Kin1-T302 occurs in *trans*. (A) The residue T281 is phosphorylated in kinase-dead mutants. Whole-cell extracts from the yeast cells expressing the wild-type Kin2^{mini} or its derivatives, as indicated in panel A, were subjected to SDS-PAGE, followed by Western blotting using T281 phosphospecific and anti-Flag antibodies. (B) *In vitro* kinase assays. Partially purified *Sc*Kin1^{mini}, *Sc*Kin2^{mini}, and *Sc*Kin2^{mini}-K128R proteins were mixed with α-casein in a kinase reaction buffer containing [γ-^{33}P]ATP. The reaction mixture was quenched after 20 min by addition of 3$\times$ SDS dye and resolved by gel electrophoresis. The gel was stained to see protein bands (lower), dried, and then subjected to autoradiography to detect the incorporation of ^{33}P in α-casein. (C) The recombinant *Ec*GST–Kin2^{mini}-T281E protein phosphorylates α-casein *in vitro*. Partially purified recombinant *Ec*GST-Kin2^{mini} (WT) or *Ec*GST–Kin2^{mini}-T281E protein was subjected to *in vitro* kinase assay using [γ-^{33}P]ATP and α-casein as a substrate. The *Ec*GST-Kin2^{mini} and α-casein protein bands are shown in the lower panel, whereas phosphate (^{33}P) incorporation in the respective α-casein and *Ec*GST-Kin2^{mini} proteins is shown in the upper panel. The asterisk indicates an unwanted protein band bound with the GST-Kin2^{mini} protein. (D) The recombinant *Ec*GST–Kin1^{mini}-T302E protein phosphorylates α-casein *in vitro*. Partially purified recombinant *Ec*GST-Kin1^{mini} (WT) or *Ec*GST–Kin1^{mini}-T302E protein was subjected to *in vitro* kinase assay using [γ-^{33}P]ATP and α-casein as a substrate. The *Ec*GST-Kin1^{mini} and α-casein protein bands are shown in the lower panel, whereas phosphate (^{33}P) incorporation in the respective α-casein and *Ec*GST-Kin1^{mini} proteins is shown in the upper panel.

cerevisiae cells by galactose (see Materials and Methods). The recombinant proteins in *Saccharomyces cerevisiae* (referred to as *Sc*Kin1^{mini}, *Sc*Kin2^{mini}, and *Sc*Kin2^{mini}-K128R) were partially purified by anti-Flag M2-agarose and subjected to *in vitro* kinase assays using α-casein as a substrate. We observed that the purified *Sc*Kin1^{mini} or *Sc*Kin2^{mini} readily phosphorylated α-casein (Fig. 7B, upper, ^{33}P, lanes 1 and 2). However, an extremely low level of α-casein phosphorylation was observed when we used *Sc*Kin2^{mini}-K128R mutant protein (Fig. 7B, upper, ^{33}P, lane 3). As shown in Fig. 4B, the Kin2^{mini}-K128R mutant did not allow the *kin1*Δ *kin2*Δ cells to grow on the tunicamycin medium (Fig. 4B, row 3). Thus, it appeared that the low level of α-casein phosphorylation was due to the presence of another kinase in the partially purified Kin2^{mini}-K128R protein. Collectively, these data confirm that *Sc*Kin2^{mini}-K128R is an inactive kinase.

We further confirmed that T281 phosphorylation occurred in a *trans* mechanism by *in vitro* kinase assay (see Materials and Methods). Initially, we made glutathione *S*-transferase (GST)-fused full-length Kin2 and Kin2^{mini} protein constructs to express full-length Kin2 (Kin2^{full}) and Kin2^{mini} (residues 94 to 526) proteins in *Escherichia coli*. However, an extremely small amount of protein was expressed from either construct. Thus, we further engineered the GST–Kin2^{mini}-94-526 construct to make a GST–Kin2-(60-526)-Δ40-ΔKI construct (D1386) (Table 2) in which 34 residues were added at the N-terminal end of GST–Kin2^{mini}-94-526 protein and the protease-labile residues 440 to

480 (i.e., 40 residues in the KER-II region) and 136 to 165 (i.e., 30 residues in the kinase domain referred here to as the kinase insert [KI]) were deleted. Interestingly, we observed that, like the Kin2^{mini} protein, the Kin2-(60-526)-Δ40-ΔKI protein was able to activate the UPR in the *kin1*Δ *kin2*Δ cells (data not shown), suggesting that Kin2-(60-526)-Δ40-ΔKI was a functional protein. Moreover, we observed that protein expression in *E. coli* from the GST–Kin2^{mini}-(60-526)-Δ40-ΔKI construct was significantly improved.

We then made two mutants of GST–Kin2^{mini}-(60-526)-Δ40-ΔKI protein: GST–Kin2^{mini}-(60-526)-Δ40-ΔKI-T281E (D1347) and GST–Kin2^{mini}-(60-526)-Δ40-ΔKI-Y275E (D1942) (Table 2). GST–Kin2^{mini}-(60-526)-Δ40-ΔKI, GST–Kin2^{mini}-(60-526)-Δ40-ΔKI-T281E and GST-Kin2^{mini}-(60-526)-Δ40-ΔKI-Y275E were expressed in *E. coli*. The recombinant proteins in *E. coli* (referred here to as *Ec*GST-Kin2^{mini}, *Ec*GST–Kin2^{mini}-T281E, and *Ec*GST–Kin2^{mini}-Y275E) were purified and mixed with the α-casein or histone in a kinase reaction buffer containing [γ-^{33}P]ATP (1 μCi per reaction). The reaction mixture was then resolved by SDS-PAGE, and the incorporation of ^{33}P in α-casein or histone (data not shown) was detected by autoradiography (Fig. 7C). A robust phosphorylation of α-casein or histone (data not shown) was observed in a reaction mixture containing GST–Kin2^{mini}-T281E protein (Fig. 7C, lane 2) but not in the reaction mixture containing *Ec*GST-Kin2^{mini} (Fig. 7C, lane 1) or *Ec*GST–Kin2^{mini}-Y275E (Fig. 7C, lane 3). These data suggested that recombinant GST–Kin2^{mini}-T281E was an active kinase, whereas the recombinant *Ec*GST-Kin2^{mini} and *Ec*GST–Kin2^{mini}-Y275E proteins were inactive kinases, likely due to lack of activating T281 phosphorylation. Collectively, our data suggest that glutamate substitution for T281, but not Y275, mimicked the phosphorylated state, thereby activating its kinase function.

We also determined by an *in vitro* kinase assay that T302 phosphorylation in Kin1 occurred by a *trans* mechanism. Initially, we made a GST-fused Kin1^{mini} protein construct to express the Kin1^{mini} protein in *E. coli*. However, the GST-Kin1^{mini} construct produced an extremely small amount of protein. Thus, we deleted the protease-labile KI region (residues A177 to I205) and expressed the GST–Kin1^{mini}-ΔKI and GST–Kin1^{mini}-ΔKI-T302E proteins. It should be noted that both Flag-tagged Kin1^{mini}-ΔKI and Kin1^{mini}-ΔKI-T302E, like Kin1^{mini}, were able to activate the UPR in the *kin1*Δ *kin2*Δ cells (data not shown), suggesting that Kin1^{mini}-ΔKI was a functional protein kinase. Moreover, we observed that protein expression in *E. coli* from the GST–Kin1^{mini}-ΔKI construct was significantly improved. The recombinant proteins in *E. coli* (referred to as *Ec*GST-Kin1^{mini} and *Ec*GST–Kin1^{mini}-T302E) were purified and subjected to *in vitro* kinase assays as described above. We observed that recombinant *Ec*GST-Kin1^{mini} was unable to phosphorylate α-casein (Fig. 7D, lane 2), likely due to a lack of activating T302 phosphorylation. However, consistent with the *Ec*GST–Kin2^{mini}-T281E protein (Fig. 7C, lane 2), *Ec*GST–Kin1^{mini}-T302E readily phosphorylated α-casein (Fig. 7D, lane 3). These data suggested that the glutamate substitution for T302 mimicked the phosphorylated state, thereby activating its kinase function. Taken together, our data suggest that phosphorylation of T281 in Kin2 or T302 in Kin1 occurs by a *trans* mechanism.

Glutamate substitution of T281 restores the defective ER-stress response associated with a mutation at the *HAC1* 3′-UTR. Since Kin kinase function has been implicated in Hac1-mediated UPR, we investigated the effect of active Kin2^{mini}-T281E protein in Hac1 expression from *HAC1* mRNA. *HAC1* mRNA consists of a short 5′-UTR, two exons (exon1 and exon2) separated by an intron, and a long 3′-UTR (52). It has been shown that an intramolecular interaction between the 5′-UTR and intron blocks translation initiation (14, 53), thereby rendering *HAC1* mRNA translationally silent (Fig. 8A). Under conditions of ER stress, *HAC1* mRNA associates with an ER-resident endonuclease, Ire1, that cleaves out the intron, thus releasing the translational block (14, 53). Recently, we have shown that a conserved sequence element (5′-G_{1140}UUGG_{1144}-3′) at the 3′-UTR makes a significant contribution to translocation, splicing, and translation of *HAC1* mRNA (31). In other words, we have shown that mutations of two consecutive guanine nucleotides (G_{1143} and G_{1144}) at the 3′-UTR reduce the UPR induction due to defects in both splicing and translation of *HAC1* mRNA, and these splicing and

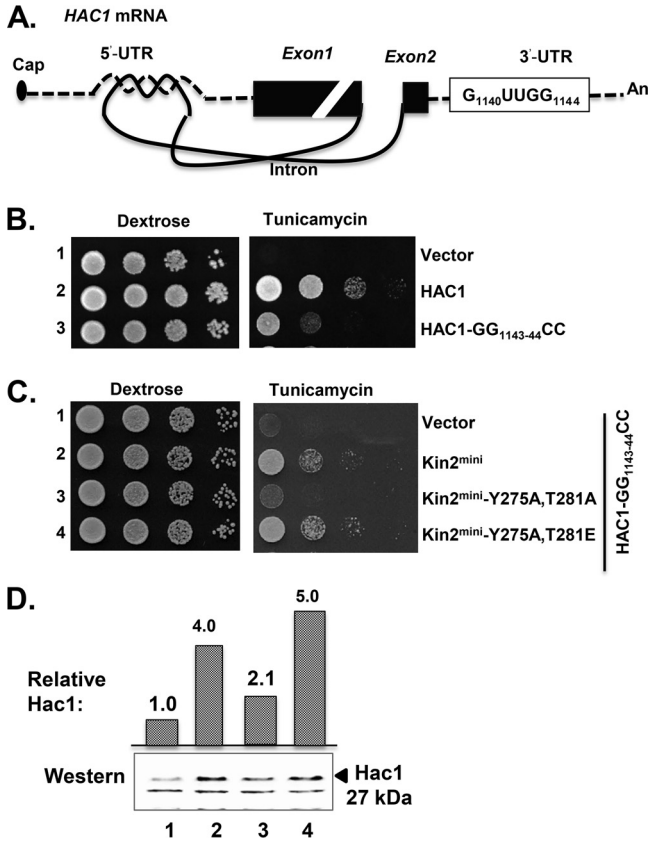

FIG 8 Thr-281 phosphorylation is required to suppress the defective alleles of *HAC1* mRNA. (A) Schematic representation of *HAC1* mRNA. The cap, 5′- and 3′-UTRs (dotted lines), exons, intron (solid line), and polyadenine (An) tail are shown. The intron has been shown to interact with its 5′-UTR. A conserved element at the 3′-UTR (i.e., 5′-$G_{1140}UUGG_{1144}$-3′) is shown. (B and C) Analysis of yeast cell growth. A *hac1*Δ *kin1*Δ deletion strain was transformed with the indicated *HAC1* or *KIN2* alleles. Transformants were then tested for growth on dextrose and tunicamycin media. (D) Analysis of Hac1 protein expression. Whole-cell extracts from the yeast cells indicated in panel C were subjected to SDS-PAGE, followed by Western blotting using an anti-Hac1 antibody. Nonspecific bands are indicated as loading controls. The relative amount of Hac1 protein (molecular size of 26.89 kDa) was estimated as a ratio of each protein band density (ImageJ software) to the lane's loading control.

translation defects can be restored by overexpressing the protein kinase Kin1 or Kin2 (31).

In order to provide further direct *in vivo* evidence that glutamate substitution of the residue T281 could activate the kinase domain, we investigated the impact of Kin2^{mini}-T281E mutant protein on Hac1-mediated UPR. The Kin2^{mini}-T281E mutant protein was overexpressed in the *kin1*Δ *hac1*Δ yeast strain containing a *HAC1-GG$_{1143-44}$CC* allele. The resulting strains were then tested for their growth on the tunicamycin medium. As shown in Fig. 8B, yeast cells expressing a *HAC1-GG$_{1143-44}$CC* allele grew more slowly on the tunicamycin medium than cells expressing a wild-type *HAC1* allele (tunicamycin, compare rows 2 and 3). The slow growth in cells was visibly more normal when Kin2^{mini} or Kin2^{mini}-Y281A,T281E, but not Kin2^{mini}-Y281A,T281A, was overexpressed from a high-copy-number vector (Fig. 8C). Western analysis showed that restoration of growth was correlated with higher levels of Hac1 protein expression (Fig. 8D, Western, compare lanes 2 and 4). These genetic and biochemical data collectively suggest that T281 phosphorylation within the activation loop of Kin2 is important for expression of Hac1 protein.

DISCUSSION

Protein kinases Kin1 and Kin2 belong to a family of serine/threonine kinases that has been shown to coordinate cellular exocytosis as well as the ER-stress response. How-

ever, it is not known how Kin kinases are activated and how they transmit stress signals to the downstream components. Here, we investigated the molecular events that lead to activation of the Kin kinase domain under conditions of ER stress. We show that both Kin1 and Kin2 proteins minimally require a kinase domain (KD) and a short adjoining kinase extension region (KER) for their function (Fig. 1). We refer these mini-functional Kin1 and Kin2 proteins as Kin1^{mini} and Kin2^{mini}, respectively. We further demonstrate that Kin2-KER is composed of two distinct subdomains (KER-I and KER-III) separated by a spacer of at least 40 amino acids (Fig. 2). The computational analyses suggest that KER-I folds and functions like an UBA-like domain by unknown mechanisms, likely maintaining the integrity of the kinase domain, as shown in the nonfermenting (Snf1)-related kinase (54).

Typically, most protein kinase domains are kept in an inactive state by means of an intramolecular interaction(s) mediated by its own domain or an intermolecular interaction(s), mediated by another subunit(s), or both (55). For example, the KA1 domain in Kin kinases functions as an autoinhibitory domain (32), whereas a regulatory subunit of PKA inhibits its kinase activity (56). The inactive kinase domain must be activated in order to perform its physiological function. Inactive-to-active transition requires release of the KD from its own domain or subunit or both. However, in many cases the isolated kinase domain is not functional. For example, we did not find any measureable Kin kinase activity when the isolated KD of Kin1 (residues 115 to 430) or Kin2 (residues 94 to 380) was expressed in yeast cells or when the purified kinase domain was subjected to an *in vitro* kinase assay using α-casein or histone as a substrate (data not shown). For the kinase activity, Kin kinases required at least an adjoining extension region (i.e., KER) outside the kinase domain. However, the structural and functional role of KER is not yet clear. Most likely, KER increases the stability of protein by promoting a specific intramolecular interaction, binds a specific partner protein that activates the kinase domain, and/or targets the protein to a specific cell compartment.

Both Kin1 and Kin2 are shown to be phosphorylated proteins. Thus, it appears that each one is regulated by a complex mechanism involving auto- and/or transphosphorylation. Mutational analyses of several phosphorylated residues revealed that the substitution of phosphomimetic glutamate for the Kin1 residue T302 or the Kin2 residues Y275 and T281 bypassed the requirement of phosphorylation in Kin1^{mini} or Kin2^{mini} proteins (Fig. 4 and 6). The Kin1 residue T302 or Kin2 residues Y275 and T281 are mapped within the activation loop of the kinase domain. Activation loop phosphorylation followed by kinase domain activation is a recurrent theme in protein kinases (57). Interestingly, we found that the Kin2 residue T281 was phosphorylated in the Kin2^{mini}-K128R and Kin2^{mini}-D248A kinase-inactive mutants (Fig. 7). Furthermore, we found that the bacterially expressed and purified GST-Kin1 or GST-Kin2 protein was unable to phosphorylate α-casein, likely due to the lack of activating T302 or T281 phosphorylation. Consistent with this, we observed that the glutamate substitution of the residue T302 in GST-Kin1 and T281 in GST-Kin2 protein led to phosphorylation of α-casein (Fig. 7). Collectively, these data suggest that phosphorylation of residue T302 in Kin1 or T281 in Kin2 occurs in a *trans* mechanism.

The Kin kinase domain shows a significant homology with the kinase domain of Snf1 (sucrose nonfermenting 1) in yeast and the AMPK (AMP-activated protein kinase)-related kinase Mark in humans. Snf1 is phosphorylated and activated by a group of three upstream kinases, Sak1, Tos3, and Elm1 (58), whereas Mark is phosphorylated and activated by an upstream kinase LKB1 complex (59). Thus, we examined the phosphorylation status of T281 residue in a yeast strain lacking all three kinases, Sak1, Tos3, and Elm1. No change in T281 phosphorylation was observed in the triple deletion strain (data not shown), suggesting that none of these kinases are involved in T281 phosphorylation. Additionally, we performed an *in vitro* kinase assay with the recombinant Kin2 protein and LKB1 complex purified from human cells. No phosphorylation of T281 in Kin2 protein was observed (data not shown). Collectively, these data suggest that T281 phosphorylation is mediated by a currently unknown kinase, which is likely

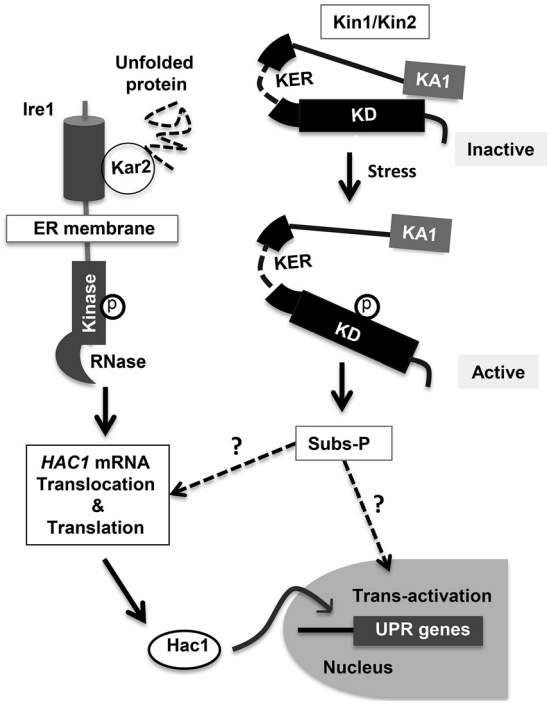

FIG 9 Proposed model for the activation of Kin kinase domain. During ER stress, unfolded proteins accumulate in the ER lumen and titrate the ER-resident protein Kar2 bound to the kinase/RNase Ire1 (left), resulting in dimerization, oligomerization, and activation of Ire1 proteins. The active Ire1 transmits the stress signal to *HAC1* mRNA, leading to its translation, which in turn activates expression of UPR genes involved in accelerating the protein-folding processes. In yeast cells, the canonical Ire1 pathway is likely synergistically activated by protein kinases Kin1 and Kin2 (right). Kin1 and Kin2 kinases are likely associated with the cellular endomembrane and/or at the cytoplasmic face of the plasma membrane. They remain in an inactive state by an intramolecular interaction between the kinase domain (KD) and the kinase-associated 1 (KA1) domain. During stress, the KD is released from the KA1 domain and is phosphorylated in *trans* by an upstream kinase. Active Kin2 then phosphorylates an unknown substrate (Subs-P) that synergistically activates the Ire1 pathway or independently transmits the stress signal to the nucleus to activate the UPR genes.

unrelated to human LKB1 or Sak1/Tos3/Elm1. Moreover, it is not known how an active Kin1 or Kin2 kinase transmits the signals by phosphorylating the downstream targets.

Recently, it was shown that the extreme C-terminal end of human Mark3, consisting of the motif KA1 and a short upstream region (referred to here as the KA1^{Mark3} domain), could drive GFP to the cellular membrane (60), suggesting that the KA1 motif plays a role in targeting the protein to the membrane. The bioinformatics analysis showed that KA1^{Mark3} is strikingly analogous to the extreme C-terminal 90 residues of Kin1 or Kin2 protein, which includes the KA1 motif (data not shown; the analogous KA1 domain of Kin2 is referred to as the KA1^{Kin2} domain). Like KA1^{Mark3}, we also found that the KA1^{Kin2} domain could target Kin2 to the plasma membrane (data not shown). From these results, it appears that Kin2 was associated with membranes where both KER and KA1 domains play important roles in membrane association.

Based on our data, together with the published results, we propose a model for Kin kinase domain activation and how Kin kinases coordinate with the Ire1 pathway to activate the ER stress response (Fig. 9). During ER stress, unfolded proteins in the ER lumen titrate the chaperone Kar2 bound to Ire1 (61), resulting in activation of both kinase and RNase domains of Ire1 through dimerization, oligomerization, and phosphorylation (62, 63). The active Ire1-RNase then cleaves the intron from *HAC1* mRNA, thereby releasing its translational block. Hac1 protein activates the expression of several protein-folding enzyme and chaperone genes. In parallel, the membrane-associated protein kinases Kin1 and Kin2 are activated by releasing their kinase domain from the autoinhibitory KA1 domain and by phosphorylating in *trans* within the

TABLE 1 Yeast strains used in this study

Yeast strain	Genotype	Reference or source
WT (BY4741)	*MAT***a** *his3-Δ1 leu2-Δ0 met5-Δ0 ura3-Δ0*	Research Genetics
kin1Δ kin2Δ strain	*MAT***a** *his3-Δ1 leu2-Δ0 met5-Δ0 ura3-Δ0 kin1::natMX kin2::kanMX*	Anshu et al. (31)
hac1Δ kin1Δ strain	*MAT***a** *his3-Δ1 leu2-Δ0 met5-Δ0 ura3-Δ0 hac1::natMX kin1::kanMX*	Anshu et al. (31)
ste2Δ strain	*MAT***a** *leu2-3,112 ura3-52 his3-Δ1 trp1 ste2::leu2 sst1-Δ5*	Stoneman et al. (46)

activation loop by an upstream kinase. Active Kin kinase then synergistically or independently activates the UPR pathway by unknown mechanisms.

Previously we have shown that, under conditions of ER stress, both GFP-Kin2 and GFP-Kin2$^{\Delta KA1}$ fusion proteins were predominantly visualized as discrete dots within the cytoplasm (31). We also found that Kin2^{mini} protein associates with endomembrane when cells are under ER stress (Fig. 3). Recently, Yuan et al. showed that Kin2 is predominantly located at the bud tip/neck (45). Thus, it appears that association of Kin2 with the membrane regulates its kinase function, and the membrane association varies depending upon the cellular conditions. Still, molecular events leading to association of Kin kinases with endomembrane in specific cellular responses remains to be established. Moreover, roles of Kin kinases in ER proteostasis raise some intriguing questions. For instance, how, when, and in what context do Kin kinases sense and transduce the ER stress signal? How do Kin kinases coordinate with the Ire1 pathway to produce an optimum UPR?

MATERIALS AND METHODS

Chemicals, reagents, and antibodies. All chemicals and reagents were purchased from commercial suppliers Sigma-Aldrich, Acros Organics, and Fisher Scientific (USA) unless otherwise noted. Restriction enzymes were purchased from NEB (New England BioLabs, USA). Protein assay reagent was obtained from Bio-Rad (USA).

Anti-Flag antibody was purchased from Sigma (F-3165). Anti-Pgk1 was purchased from Thermo Fisher Scientific, USA (459250). Antiactin was purchased from Santa Cruz, USA (sc-47778). Anti-GST was purchased from Invitrogen (13-6700). We raised a polyclonal antibody against the recombinant Hac1 protein from Thermo Fisher Scientific (USA). We raised an antibody against a T281 phospho-specific peptide (RKQLHpTFCGS [pT, phopshorylated threonine]) from GenScript, USA.

Yeast strains and growth conditions. Yeast cells were grown and cultured at 30°C on a standard liquid YPD (yeast extract-peptone-dextrose containing 1% yeast extract, 1% peptone, and 2% glucose) and/or SC (synthetic complete containing 1.44 g/liter yeast nitrogen base without amino acids, 5 g/liter ammonium sulfate, amino acid supplement, and 2% glucose) medium or on a standard solid YPD or SC medium (containing 2% agar).

To monitor cell growth on a solid SC-uracil medium (SC medium without uracil) containing tunicamycin (2.0 μg/ml), the following methods were used. Cells were suspended in sterile water and diluted to an optical density at 600 nm (OD_{600}) of ~0.5. The cells then were serially diluted to 10^{-1}, 10^{-2}, and 10^{-3}. Samples (5 μl) of each dilution were spotted on the solid medium and incubated at 30°C for 48 h. The yeast strains used in these studies are listed in Table 1.

Bacterial strains and plasmids. Standard gene cloning and genetic engineering techniques were used for gene mutations and generation of plasmids. All constructs were verified by DNA sequencing. Four standard plasmids were used in this study: (i) D1 (pRS313), a low-copy-number *HIS*-marked plasmid; (ii) D8 (pRS426), a high-copy-number *URA3*-marked 2μ plasmid; (iii) D18 (pEMBLyex4), a high-copy-number *URA3*-marked 2μ plasmid for yeast protein expression; and (iv) D1163 (pGEX-2T-TEV), a bacterial expression vector. The plasmids used in this study are listed in Table 2.

Purification of Kin1 or Kin2 protein from yeast and bacteria. The *kin1Δ kin2Δ* yeast cells containing the *URA3*-marked plasmid expressing a Flag-tagged Kin1 or Kin2 protein were grown overnight in liquid SC-uracil medium. The overnight culture was resuspended in fresh medium to give an OD_{600} of ~0.1 and grown further until the OD_{600} reached ~0.8 to 1.0. Cells were then harvested and grown for another 8 h in liquid SGR-uracil (synthetic complete medium containing 10% galactose and 2% raffinose supplemented with required nutrients without dextrose and uracil). Cells were harvested and the Flag-tagged recombinant protein was purified by Flag M2-agarose slurry (M8823; Sigma, USA) using the standard protocol.

BL21(DE3) pLysS *E. coli* cells containing a plasmid expressing the GST-Kin1 or GST-Kin2 protein were grown overnight in LB medium. The overnight culture was resuspended in fresh LB medium to give an OD_{600} of ~0.1 and grown further until the OD_{600} reached ~0.6 to 0.8. Isopropyl-β-D-1-thiogalactopyranoside (IPTG) then was added to the bacterial culture (final concentration, 0.5 mM) and grown further for another 16 h at 25°C at 200 rpm/min. Cells were harvested and the recombinant GST-tagged Kin1 or Kin2 protein was purified by GST-agarose beads (17-0756-01; GE Healthcare, USA) using the standard protocol.

TABLE 2 Plasmids used in this study

Plasmid	Detail(s)	Reference or source
D1	pRS313, low-copy-no. *HIS3* vector	
D8	pRS426, high-copy-no. *URA3* vector	
D18	pEMBLyeX4 expression vector	
D197	Kin2 in 2μ *URA3* vector	Patrick Brennwald
D619	Kin1 in pBG1805 expression vector	Benjamin Turk
D1163	pGEX-2T-TEV HTa expression vector	
D1400	Kin2-(1-1147) in D18	This study
D1129	Kin2-(94-526) in D18	Anshu et al. (31)
D1186	Kin2-(94-400) in D18	This study
D1184	Kin2-(94-440) in D18	This study
D1182	Kin2-(94-480) in D18	This study
D1220	Kin2-(94-526)-Δ(400-440) in D18	This study
D1191	Kin2-(94-526)-Δ(440-480) in D18	This study
D1742	Kin2-(94-510) in D18	This study
D1181	Kin2-(94-500) in D18	This study
D1221	Kin2-(94-526)-D248A in D18	This study
D1239	Kin2-(94-526)-Y275A,T281A in D18	This study
D1514	Kin2-(94-526)-Y275A,T281E in D18	This study
D1353	Kin1-KD in D18	This study
D1534	Kin1 (115-515)-Y294F,S296A,T302A in D18	This study
D1535	Kin1 (115-515)-Y294F,S296A,T302E in D18	This study
D1507	Kin2-(94-526)-K128R in D18	This study
D1386	Kin2-(60-526)-Δ40, ΔKI in D1163	This study
D1347	Kin2-(60-526)-Δ40, ΔKI, T281E in D1163	This study
D1688	Hac1 WT in D1	This study
D1689	Hac1 $GG_{1143-1144}CC$ in D1	This study
D1459	GFP-Kin2-(1-526) in D8	This study
D1258	GFP-KA1 in D8	This study
D1882	Kin1-(115-430) in D18	This study
D1963	Ste2-YFP in a high-copy-no. *TRP1* vector	Stoneman et al. (46)
D1237	Kin2-(94-526)-Y275A in D18	This study
D1238	Kin2-(94-526)-T281A in D18	This study
D1570	Kin2-(94-526)-Y275E,T281A in D18	This study
D852	Kin2 in D8	This study
D853	Kin2-D248A in D8	This study
D1950	Kin2-T281A in D8	This study
D1949	Kin2-Y275A in D8	This study
D1946	Kin2-Y275A,T281A in D8	This study
D1947	Kin2-Y275E,T281A in D8	This study
D1948	Kin2-Y275A,T281E in D8	This study
D1968	Kin1-(115-515)-D269A in D18	This study
D1955	Kin1-(115-515)-S296E,T302A in D18	This study
D1942	Kin2-(60-526)-Δ40, ΔKI, Y275E in D1163	This study
D1379	Kin1-(58-515)-ΔKI in D1163	This study
D1380	Kin1-(58-515)-ΔKI, T302E in D1163	This study

Preparation of whole-cell extract and Western blot analysis. Yeast cells were grown overnight in a liquid SC-uracil medium. The cells grown overnight were resuspended in a fresh SC-uracil medium to give an OD_{600} of ~0.1 and further grown for another 3 to 4 h to reach an OD_{600} of ~0.6 to 0.8. Cells were then harvested by centrifugation at 3,000 rpm for 10 min and resuspended in SGR medium (10% galactose and 2% raffinose supplemented with required nutrients) and grown further for another 8 h. Cells at an OD_{600} of approximately 10 were taken, and total cellular proteins were precipitated by adding 200 μl of 100% trichloroacetic acid (TCA) overnight at 4°C. From the TCA-precipitated cellular proteins, whole-cell extracts (WCE) were prepared as described previously (31). WCEs were separated by SDS-PAGE and subjected to Western blot analyses with an appropriate antibody. Each Western blot analysis was repeated at least twice, and representative data are shown.

Mass spectrometric analysis. Yeast cells expressing the Flag-$Kin2^{mini}$ protein were grown overnight in a liquid SC-uracil medium. The overnight culture was resuspended in a fresh liquid SC-uracil medium and grown until the OD_{600} reached ~0.8 to 1. Cells were harvested and resuspended in SGR-uracil medium and grown for 8 h. Tunicamycin (2.0 μg/ml) was added to the culture and grown for another 2 h. Cells were harvested and lysed in a buffer containing 20 mM Tris-HCl, pH 7.5, 500 mM NaCl, 300 mM NH_4SO_4, 1 mM phenylmethylsulfonyl fluoride (PMSF), 1 mM NaF, 15 mM β-glycerophosphate, 1 mM $NaOVa_4$, 0.1% Triton X-100, and Pierce protease inhibitor tablet (1 tablet for 25 ml buffer). Whole-cell lysate was prepared by centrifugation at 14,000 rpm for 10 min. Flag M2-agarose slurry (Sigma) was equilibrated with the same buffer. Whole-cell lysate was incubated with the Flag M2-agarose beads for 1 h. Beads were washed with the same buffer. Flag-Kin2 protein was eluted with the Flag peptide (0.1

mg/ml). Purified Flag-Kin2 protein was run on SDS-PAGE. The Kin2 protein band was detected by Coomassie stain. The stained Kin2 protein band was cut and sent to the Madison Mass Spectrometry Facility, which identified 5 major phosphorylated residues in three peptides by matrix-assisted laser desorption ionization–tandem time of flight mass spectrometry after in-gel digestion: QHSLPSPKNEpSE ILER (residues 141 to 156), SNIFDpYRKQLHpTFCG (residues 270 to 285), and DDENpSpSILHEK (residues 324 to 335).

***In vitro* kinase assay.** The partially purified Kin2 and histone or dephosphorylated form of α-casein (C6780; Sigma, USA) proteins were mixed with the γ-^{33}P-labelled ATP (1 μCi per reaction) in a kinase reaction buffer (20 mM Tris-HCl, pH 8.0, 50 mM KCl, 25 mM $MgCl_2$, 10% glycerol, 1 mM DTT) for 20 min at room temperature. The kinase reaction was stopped by 3× SDS dye (NEB). The reaction mixture was separated by SDS-PAGE. The protein gel was fixed for an hour in a fixing solution (50% methanol and 10% glacial acetic acid), stained for 20 min in a staining solution (0.1% Coomassie brilliant blue R-250, 50% methanol, and 10% glacial acetic acid), and destained overnight in a destaining solution (40% methanol and 10% glacial acetic acid). The gel was dried and autoradiographed with a phosphorimager to detect the ^{33}P.

***In vivo* imaging of yeast cells by a two-photon microspectroscope.** The GFP2 and YFP signals were detected in the *ste2*Δ cells expressing Kin2-GFP2 and Ste2-YFP, either separately or together, using a two-photon microspectroscope comprised of a Nikon Eclipse Ti (Nikon Instruments, Inc., Melville, NY) inverted microscope stand and a modified OptiMiS scanning/detection head from Aurora Spectral Technologies (Grafton, WI). Excitation was performed using a mode-locked, pulsed laser (MaiTai; Spectra Physics, Santa Clara, CA) with wavelengths tunable between 690 nm and 1,040 nm using a line-scan protocol. Excitation light, shaped in the form of a line, was focused using an infinity-corrected, Plan-Apochromat, oil immersion objective (100×; numerical aperture of 1.45; Nikon Instruments, Inc.). The emitted light was collected using the same objective, passed through a transmission grating for spectral resolution, and detected with a cooled electron-multiplying charge-coupled device camera (iXon X3 897; Andor Technologies, Belfast, UK). The spatial dimensions of the acquired images were 440 by 300 pixels, and detection bandwidth ranged from 430 to 630 nm with a resolution of 5 nm.

Yeast cells were grown in SC-uracil-tryptophan medium until an OD_{600} of ~0.6. The DTT then was added to the culture medium in order to induce ER stress. Cells (10 μl) expressing only Ste2-YFP was placed onto glass slides, covered with a coverslip, and scanned with an optical microspectroscope using a 920-nm light wavelength at 1.1 mW/pixel. Similarly, cells expressing only Kin2-GFP2 were imaged following excitation using an 800-nm wavelength at 1.11 mW/pixel. The preliminary scans were used to determine elementary spectra and then used in subsequent analysis of cells coexpressing Ste2-YFP and Kin2-GFP2, which were imaged by following the same procedure, using a first excitation at 800 nm and then one at 920 nm at identical power/pixel. Both excitation wavelengths produced the emissions from both GFP2 and YFP in different proportions, so spectral unmixing of these samples was performed utilizing a general least-squares algorithm in order to determine the relative abundance of each spectrum (64). Arbitrary intensity of each elementary spectrum was multiplied by their respective spectral integral to give the number of photons given off by the fluorophore in a sample. The unmixed signals were denoted by false colors (yellow to Ste2-YFP and green to Kin2-GFP2), and the resulting images were overlaid to observe their colocalization. Averages and variances computed for each image were used to generate final weighted averages and standard errors via standard mathematical procedures.

Membrane fractionation. Yeast cells expressing the Flag-Kin2^{mini} protein from a *URA3*-marked plasmid were grown in liquid SC-uracil medium until the OD_{600} reached ~0.6 to 0.8. Cells were collected by centrifugation at 3,000 rpm for 10 min, resuspended in SGR-uracil medium, and allowed to grow for another 4 h. Cells (OD_{600} of 10) were harvested and lysed by glass beads in 400 μl of lysis buffer containing 25 mM Tris-phosphate, pH 6.7, 1 mM β-mercaptoethanol (β-ME), 1 mM PMSF, and 1 protease tablet per 25 ml buffer. The whole-cell lysate was clarified by centrifugation at 5,000 rpm (2,655 × *g*) for 10 min at 4°C. The clear supernatant was divided into two separate tubes (150 μl each). The first tube with 150 μl of lysate was used to precipitate the total soluble and insoluble proteins as follows. A volume of 37.5 μl of 100% TCA was added and kept on ice for 10 min. Total protein was collected by centrifugation at 6,000 rpm for 10 min and solubilized in a buffer (40 μl of 1 M Tris-HCl, pH 8.0, and 10 μl of 5× SDS dye) at 90°C. This fraction was considered the input.

The second tube, containing 150 μl of lysate, was further centrifuged at 14,000 rpm (20,817 × *g*) for 30 min at 4°C in order to pellet the insoluble fraction (the membrane fraction). The supernatant containing the soluble proteins was then collected in a fresh tube, and total protein was precipitated and solubilized in a buffer as described above (the soluble protein fraction). The pellet containing the insoluble membrane fraction was solubilized in a buffer (40 μl of Tris-HCl, pH 8.0, and 10 μl of 5× SDS dye) at 90°C. The input (1/2), soluble, and insoluble protein fractions were subjected to Western analysis.

The pellet containing the membrane fraction was also solubilized in a buffer (50 mM Tris-HCl, pH 8.0, and 1 mM DTT) containing 0, 0.5, or 1% Triton X-100. The pellet and supernatant fractions were separated by centrifugation at 14,000 rpm for 20 min at 4°C. The pellet and supernatant fractions were then separated by SDS-PAGE and subjected to Western blot analyses using an anti-Flag antibody.

ACKNOWLEDGMENTS

This work was supported by a grant to M.D. from the U.S. National Institutes of Health (1R01GM124183). This research was also supported in part by grants to V.R. from the U.S. National Science Foundation Major Research Instrumentation Program

(PHY-1126386 and PHY-1626450) and the UWM Research Growth Initiative (101X333 and 101X340).

We thank Benjamin E. Turk (Yale University School of Medicine, New Haven, CT) and Patrick Brennwald (UNC School of Medicine, Chapel Hill, NC) for reagents and/or helpful discussion throughout the project.

REFERENCES

1. Schwarz DS, Blower MD. 2016. The endoplasmic reticulum: structure, function and response to cellular signaling. Cell Mol Life Sci 73:79–94. https://doi.org/10.1007/s00018-015-2052-6.
2. English AR, Voeltz GK. 2013. Endoplasmic reticulum structure and interconnections with other organelles. Cold Spring Harb Perspect Biol 5:a013227. https://doi.org/10.1101/cshperspect.a013227.
3. Zimmermann R, Eyrisch S, Ahmad M, Helms V. 2011. Protein translocation across the ER membrane. Biochim Biophys Acta 1808:912–924. https://doi.org/10.1016/j.bbamem.2010.06.015.
4. Schroder M. 2008. Endoplasmic reticulum stress responses. Cell Mol Life Sci 65:862–894. https://doi.org/10.1007/s00018-007-7383-5.
5. Walter P, Ron D. 2011. The unfolded protein response: from stress pathway to homeostatic regulation. Science 334:1081–1086. https://doi.org/10.1126/science.1209038.
6. Ron D, Walter P. 2007. Signal integration in the endoplasmic reticulum unfolded protein response. Nat Rev Mol Cell Biol 8:519–529. https://doi.org/10.1038/nrm2199.
7. Wang XZ, Harding HP, Zhang Y, Jolicoeur EM, Kuroda M, Ron D. 1998. Cloning of mammalian Ire1 reveals diversity in the ER stress responses. EMBO J 17:5708–5717. https://doi.org/10.1093/emboj/17.19.5708.
8. Tirasophon W, Welihinda AA, Kaufman RJ. 1998. A stress response pathway from the endoplasmic reticulum to the nucleus requires a novel bifunctional protein kinase/endoribonuclease (Ire1p) in mammalian cells. Genes Dev 12:1812–1824. https://doi.org/10.1101/gad.12.12.1812.
9. Sidrauski C, Walter P. 1997. The transmembrane kinase Ire1p is a site-specific endonuclease that initiates mRNA splicing in the unfolded protein response. Cell 90:1031–1039. https://doi.org/10.1016/S0092-8674(00)80369-4.
10. Harding HP, Zhang Y, Ron D. 1999. Protein translation and folding are coupled by an endoplasmic-reticulum-resident kinase. Nature 397:271–274. https://doi.org/10.1038/16729.
11. Haze K, Yoshida H, Yanagi H, Yura T, Mori K. 1999. Mammalian transcription factor ATF6 is synthesized as a transmembrane protein and activated by proteolysis in response to endoplasmic reticulum stress. Mol Biol Cell 10:3787–3799. https://doi.org/10.1091/mbc.10.11.3787.
12. Cox JS, Shamu CE, Walter P. 1993. Transcriptional induction of genes encoding endoplasmic reticulum resident proteins requires a transmembrane protein kinase. Cell 73:1197–1206. https://doi.org/10.1016/0092-8674(93)90648-A.
13. Cox JS, Walter P. 1996. A novel mechanism for regulating activity of a transcription factor that controls the unfolded protein response. Cell 87:391–404. https://doi.org/10.1016/S0092-8674(00)81360-4.
14. Ruegsegger U, Leber JH, Walter P. 2001. Block of HAC1 mRNA translation by long-range base pairing is released by cytoplasmic splicing upon induction of the unfolded protein response. Cell 107:103–114. https://doi.org/10.1016/S0092-8674(01)00505-0.
15. Nojima H, Leem SH, Araki H, Sakai A, Nakashima N, Kanaoka Y, Ono Y. 1994. Hac1: a novel yeast bZIP protein binding to the CRE motif is a multicopy suppressor for cdc10 mutant of Schizosaccharomyces pombe. Nucleic Acids Res 22:5279–5288. https://doi.org/10.1093/nar/22.24.5279.
16. Chapman RE, Walter P. 1997. Translational attenuation mediated by an mRNA intron. Curr Biol 7:850–859. https://doi.org/10.1016/S0960-9822(06)00373-3.
17. Lu SJ, Yang ZT, Sun L, Sun L, Song ZT, Liu JX. 2012. Conservation of IRE1-regulated bZIP74 mRNA unconventional splicing in rice (Oryza sativa L.) involved in ER stress responses. Mol Plant 5:504–514. https://doi.org/10.1093/mp/ssr115.
18. Deng Y, Humbert S, Liu JX, Srivastava R, Rothstein SJ, Howell SH. 2011. Heat induces the splicing by IRE1 of a mRNA encoding a transcription factor involved in the unfolded protein response in Arabidopsis. Proc Natl Acad Sci U S A 108:7247–7252. https://doi.org/10.1073/pnas.1102117108.
19. Calfon M, Zeng H, Urano F, Till JH, Hubbard SR, Harding HP, Clark SG, Ron D. 2002. IRE1 couples endoplasmic reticulum load to secretory capacity by processing the XBP-1 mRNA. Nature 415:92–96. https://doi.org/10.1038/415092a.
20. Yanagitani K, Kimata Y, Kadokura H, Kohno K. 2011. Translational pausing ensures membrane targeting and cytoplasmic splicing of XBP1u mRNA. Science 331:586–589. https://doi.org/10.1126/science.1197142.
21. Sidrauski C, Cox JS, Walter P. 1996. tRNA ligase is required for regulated mRNA splicing in the unfolded protein response. Cell 87:405–413. https://doi.org/10.1016/S0092-8674(00)81361-6.
22. Lu Y, Liang FX, Wang X. 2014. A synthetic biology approach identifies the mammalian UPR RNA ligase RtcB. Mol Cell 55:758–770. https://doi.org/10.1016/j.molcel.2014.06.032.
23. Hinnebusch AG. 2005. Translational regulation of GCN4 and the general amino acid control of yeast. Annu Rev Microbiol 59:407–450. https://doi.org/10.1146/annurev.micro.59.031805.133833.
24. Harding HP, Novoa I, Zhang Y, Zeng H, Wek R, Schapira M, Ron D. 2000. Regulated translation initiation controls stress-induced gene expression in mammalian cells. Mol Cell 6:1099–1108. https://doi.org/10.1016/S1097-2765(00)00108-8.
25. Olzmann JA, Kopito RR, Christianson JC. 2013. The mammalian endoplasmic reticulum-associated degradation system. Cold Spring Harb Perspect Biol 5:a013185. https://doi.org/10.1101/cshperspect.a013185.
26. Qi L, Tsai B, Arvan P. 2017. New insights into the physiological role of endoplasmic reticulum-associated degradation. Trends Cell Biol 27:430–440. https://doi.org/10.1016/j.tcb.2016.12.002.
27. Thibault G, Ng DT. 2012. The endoplasmic reticulum-associated degradation pathways of budding yeast. Cold Spring Harb Perspect Biol 4:a013193. https://doi.org/10.1101/cshperspect.a013193.
28. Chen Y, Feldman DE, Deng C, Brown JA, De Giacomo AF, Gaw AF, Shi G, Le QT, Brown JM, Koong AC. 2005. Identification of mitogen-activated protein kinase signaling pathways that confer resistance to endoplasmic reticulum stress in Saccharomyces cerevisiae. Mol Cancer Res 3:669–677. https://doi.org/10.1158/1541-7786.MCR-05-0181.
29. Winnay JN, Dirice E, Liew CW, Kulkarni RN, Kahn CR. 2014. p85alpha deficiency protects beta-cells from endoplasmic reticulum stress-induced apoptosis. Proc Natl Acad Sci U S A 111:1192–1197. https://doi.org/10.1073/pnas.1322564111.
30. Park SW, Zhou Y, Lee J, Lu A, Sun C, Chung J, Ueki K, Ozcan U. 2010. The regulatory subunits of PI3K, p85alpha and p85beta, interact with XBP-1 and increase its nuclear translocation. Nat Med 16:429–437. https://doi.org/10.1038/nm.2099.
31. Anshu A, Mannan MA, Chakraborty A, Chakrabarti S, Dey M. 2015. A novel role for protein kinase Kin2 in regulating HAC1 mRNA translocation, splicing, and translation. Mol Cell Biol 35:199–210. https://doi.org/10.1128/MCB.00981-14.
32. Elbert M, Rossi G, Brennwald P. 2005. The yeast par-1 homologs kin1 and kin2 show genetic and physical interactions with components of the exocytic machinery. Mol Biol Cell 16:532–549. https://doi.org/10.1091/mbc.e04-07-0549.
33. Drewes G, Ebneth A, Preuss U, Mandelkow EM, Mandelkow E. 1997. MARK, a novel family of protein kinases that phosphorylate microtubule-associated proteins and trigger microtubule disruption. Cell 89:297–308. https://doi.org/10.1016/S0092-8674(00)80208-1.
34. Guo S, Kemphues KJ. 1995. par-1, a gene required for establishing polarity in C. elegans embryos, encodes a putative Ser/Thr kinase that is asymmetrically distributed. Cell 81:611–620. https://doi.org/10.1016/0092-8674(95)90082-9.
35. Tassan JP, Le Goff X. 2004. An overview of the KIN1/PAR-1/MARK kinase family. Biol Cell 96:193–199. https://doi.org/10.1016/j.biolcel.2003.10.009.
36. Drewes G, Nurse P. 2003. The protein kinase kin1, the fission yeast orthologue of mammalian MARK/PAR-1, localises to new cell ends after

mitosis and is important for bipolar growth. FEBS Lett 554:45–49. https://doi.org/10.1016/S0014-5793(03)01080-9.
37. Shulman JM, Benton R, St Johnston D. 2000. The Drosophila homolog of C. elegans PAR-1 organizes the oocyte cytoskeleton and directs oskar mRNA localization to the posterior pole. Cell 101:377–388. https://doi.org/10.1016/S0092-8674(00)80848-X.
38. Biernat J, Wu YZ, Timm T, Zheng-Fischhofer Q, Mandelkow E, Meijer L, Mandelkow EM. 2002. Protein kinase MARK/PAR-1 is required for neurite outgrowth and establishment of neuronal polarity. Mol Biol Cell 13:4013–4028. https://doi.org/10.1091/mbc.02-03-0046.
39. Knighton DR, Zheng JH, Ten Eyck LF, Xuong NH, Taylor SS, Sowadski JM. 1991. Structure of a peptide inhibitor bound to the catalytic subunit of cyclic adenosine monophosphate-dependent protein kinase. Science 253:414–420. https://doi.org/10.1126/science.1862343.
40. Walinda E, Morimoto D, Sugase K, Konuma T, Tochio H, Shirakawa M. 2014. Solution structure of the ubiquitin-associated (UBA) domain of human autophagy receptor NBR1 and its interaction with ubiquitin and polyubiquitin. J Biol Chem 289:13890–13902. https://doi.org/10.1074/jbc.M114.555441.
41. Murphy JM, Korzhnev DM, Ceccarelli DF, Briant DJ, Zarrine-Afsar A, Sicheri F, Kay LE, Pawson T. 2007. Conformational instability of the MARK3 UBA domain compromises ubiquitin recognition and promotes interaction with the adjacent kinase domain. Proc Natl Acad Sci U S A 104:14336–14341. https://doi.org/10.1073/pnas.0703012104.
42. Goldberg J, Nairn AC, Kuriyan J. 1996. Structural basis for the autoinhibition of calcium/calmodulin-dependent protein kinase I. Cell 84:875–887. https://doi.org/10.1016/S0092-8674(00)81066-1.
43. Shvartsman DE, Donaldson JC, Diaz B, Gutman O, Martin GS, Henis YI. 2007. Src kinase activity and SH2 domain regulate the dynamics of Src association with lipid and protein targets. J Cell Biol 178:675–686. https://doi.org/10.1083/jcb.200701133.
44. Tibbetts M, Donovan M, Roe S, Stiltner AM, Hammond CI. 1994. KIN1 and KIN2 protein kinases localize to the cytoplasmic face of the yeast plasma membrane. Exp Cell Res 213:93–99. https://doi.org/10.1006/excr.1994.1177.
45. Yuan SM, Nie WC, He F, Jia ZW, Gao XD. 2016. Kin2, the budding yeast ortholog of animal MARK/PAR-1 kinases, localizes to the sites of polarized growth and may regulate septin organization and the cell wall. PLoS One 11:e0153992. https://doi.org/10.1371/journal.pone.0153992.
46. Stoneman MR, Paprocki JD, Biener G, Yokoi K, Shevade A, Kuchin S, Raicu V. 2017. Quaternary structure of the yeast pheromone receptor Ste2 in living cells. Biochim Biophys Acta 1859:1456–1464. https://doi.org/10.1016/j.bbamem.2016.12.008.
47. Huse M, Kuriyan J. 2002. The conformational plasticity of protein kinases. Cell 109:275–282. https://doi.org/10.1016/S0092-8674(02)00741-9.
48. Lamb A, Tibbetts M, Hammond CI. 1991. The product of the KIN1 locus in Saccharomyces cerevisiae is a serine/threonine-specific protein kinase. Yeast 7:219–228. https://doi.org/10.1002/yea.320070304.
49. Beenstock J, Mooshayef N, Engelberg D. 2016. How do protein kinases take a selfie (autophosphorylate)? Trends Biochem Sci 41:938–953. https://doi.org/10.1016/j.tibs.2016.08.006.
50. Cheng X, Ma Y, Moore M, Hemmings BA, Taylor SS. 1998. Phosphorylation and activation of cAMP-dependent protein kinase by phosphoinositide-dependent protein kinase. Proc Natl Acad Sci U S A 95:9849–9854.
51. Cameron AJ, Escribano C, Saurin AT, Kostelecky B, Parker PJ. 2009. PKC maturation is promoted by nucleotide pocket occupation independently of intrinsic kinase activity. Nat Struct Mol Biol 16:624–630. https://doi.org/10.1038/nsmb.1606.
52. Nagalakshmi U, Wang Z, Waern K, Shou C, Raha D, Gerstein M, Snyder M. 2008. The transcriptional landscape of the yeast genome defined by RNA sequencing. Science 320:1344–1349. https://doi.org/10.1126/science.1158441.
53. Sathe L, Bolinger C, Mannan MA, Dever TE, Dey M. 2015. Evidence that base-pairing interaction between intron and mRNA leader sequences inhibits initiation of HAC1 mRNA translation in yeast. J Biol Chem 290:21821–21832. https://doi.org/10.1074/jbc.M115.649335.
54. Wang YL, Wang J, Chen X, Wang ZX, Wu JW. 2018. Crystal structure of the kinase and UBA domains of SNRK reveals a distinct UBA binding mode in the AMPK family. Biochem Biophys Res Commun 495:1–6. https://doi.org/10.1016/j.bbrc.2017.10.105.
55. Johnson LN, Noble ME, Owen DJ. 1996. Active and inactive protein kinases: structural basis for regulation. Cell 85:149–158. https://doi.org/10.1016/S0092-8674(00)81092-2.
56. Wiley JC, Wailes LA, Idzerda RL, McKnight GS. 1999. Role of regulatory subunits and protein kinase inhibitor (PKI) in determining nuclear localization and activity of the catalytic subunit of protein kinase A. J Biol Chem 274:6381–6387. https://doi.org/10.1074/jbc.274.10.6381.
57. Nolen B, Taylor S, Ghosh G. 2004. Regulation of protein kinases; controlling activity through activation segment conformation. Mol Cell 15:661–675. https://doi.org/10.1016/j.molcel.2004.08.024.
58. Hong SP, Leiper FC, Woods A, Carling D, Carlson M. 2003. Activation of yeast Snf1 and mammalian AMP-activated protein kinase by upstream kinases. Proc Natl Acad Sci U S A 100:8839–8843. https://doi.org/10.1073/pnas.1533136100.
59. Lizcano JM, Goransson O, Toth R, Deak M, Morrice NA, Boudeau J, Hawley SA, Udd L, Makela TP, Hardie DG, Alessi DR. 2004. LKB1 is a master kinase that activates 13 kinases of the AMPK subfamily, including MARK/PAR-1. EMBO J 23:833–843. https://doi.org/10.1038/sj.emboj.7600110.
60. Moravcevic K, Mendrola JM, Schmitz KR, Wang YH, Slochower D, Janmey PA, Lemmon MA. 2010. Kinase associated-1 domains drive MARK/PAR1 kinases to membrane targets by binding acidic phospholipids. Cell 143:966–977. https://doi.org/10.1016/j.cell.2010.11.028.
61. Normington K, Kohno K, Kozutsumi Y, Gething MJ, Sambrook J. 1989. S. cerevisiae encodes an essential protein homologous in sequence and function to mammalian BiP. Cell 57:1223–1236. https://doi.org/10.1016/0092-8674(89)90059-7.
62. Lee KP, Dey M, Neculai D, Cao C, Dever TE, Sicheri F. 2008. Structure of the dual enzyme Ire1 reveals the basis for catalysis and regulation in nonconventional RNA splicing. Cell 132:89–100. https://doi.org/10.1016/j.cell.2007.10.057.
63. Korennykh AV, Egea PF, Korostelev AA, Finer-Moore J, Zhang C, Shokat KM, Stroud RM, Walter P. 2009. The unfolded protein response signals through high-order assembly of Ire1. Nature 457:687–693. https://doi.org/10.1038/nature07661.
64. Patowary S, Pisterzi LF, Biener G, Holz JD, Oliver JA, Wells JW, Raicu V. 2015. Experimental verification of the kinetic theory of FRET using optical microspectroscopy and obligate oligomers. Biophys J 108:1613–1622. https://doi.org/10.1016/j.bpj.2015.02.021.